Optical Properties of Atmospheric Aerosol in Maritime Environments

ALEXANDER SMIRNOV,* BRENT N. HOLBEN,+ YORAM J. KAUFMAN,# OLEG DUBOVIK,* THOMAS F. ECK,@ ILYA SLUTSKER,* CHRISTOPHE PIETRAS,& AND RANGASAYI N. HALTHORE**,++

*Science Systems and Applications, Inc., and NASA Goddard Space Flight Center, Greenbelt, Maryland
+Biospheric Sciences Branch, NASA Goddard Space Flight Center, Greenbelt, Maryland
#Climate and Radiation Branch, NASA Goddard Space Flight Center, Greenbelt, Maryland
@Goddard Environmental Science and Technology Center, University of Maryland Baltimore County, Baltimore, Maryland, and NASA Goddard Space Flight Center, Greenbelt, Maryland
&Science Applications International Corporation, and NASA Goddard Space Flight Center, Greenbelt, Maryland
**Department of Applied Science, Brookhaven National Laboratory, Upton, New York

(Manuscript received 13 December 2000, in final form 15 May 2001)

ABSTRACT

Systematic characterization of aerosol over the oceans is needed to understand the aerosol effect on climate and on transport of pollutants between continents. Reported are the results of a comprehensive optical and physical characterization of ambient aerosol in five key island locations of the Aerosol Robotic Network (AERONET) of sun and sky radiometers, spanning over 2–5 yr. The results are compared with aerosol optical depths and size distributions reported in the literature over the last 30 yr. Aerosol found over the tropical Pacific Ocean (at three sites between 20°S and 20°N) still resembles mostly clean background conditions dominated by maritime aerosol. The optical thickness is remarkably stable with mean value of $\tau_a(500\text{ nm}) = 0.07$, mode value at $\tau_{am} = 0.06$, and standard deviation of 0.02–0.05. The average Ångström exponent range, from 0.3 to 0.7, characterizes the wavelength dependence of the optical thickness. Over the tropical to subtropical Atlantic (two stations at 7°S and 32°N) the optical thickness is significantly higher: $\tau_a(500\text{ nm}) = 0.14$ and $\tau_{am} = 0.10$ due to the frequent presence of dust, smoke, and urban–industrial aerosol. For both oceans the atmospheric column aerosol is characterized by a bimodal lognormal size distribution with a fine mode at effective radius $R_{\text{eff}} = 0.11 \pm 0.01$ μm and coarse mode at $R_{\text{eff}} = 2.1 \pm 0.3$ μm. A review of the published 150 historical ship measurements from the last three decades shows that τ_{am} was around 0.07 to 0.12 in general agreement with the present finding. The information should be useful as a test bed for aerosol global models and aerosol representation in global climate models. With global human population expansion and industrialization, these measurements can serve in the twenty-first century as a basis to assess decadal changes in the aerosol concentration, properties, and radiative forcing of climate.

1. Introduction

Aerosol science returned to prominence in the last decade due to clear evidence of anthropogenic impacts and the important role of aerosols in the radiative forcing of climate. It became evident that in order to understand the effect of greenhouse gases on past climates and on future climate change (e.g., Hansen et al. 2000) we need accurate information on aerosol optical properties (Penner et al. 1994) and their direct and indirect (through cloud modification) interaction with the solar and thermal radiation (Twomey 1984; Charlson et al. 1992; IPCC 1994). The variety of aerosol sources both natural and anthropogenic, and the short lifetime of aerosols (5–10 days) results in a spatially and temporally heterogeneous aerosol field, making aerosol characterization and modeling a real challenge. To characterize this diversity there have been a flurry of field experiments in the last decade [e.g., heavy smoke aerosol in South America—Smoke, Clouds, and Radiation-Brazil (Kaufman et al. 1998); pollution from the eastern United States—Tropospheric Aerosol Radiative Forcing Observational Experiment (Russell et al. 1999); clean maritime aerosol—First Aerosol Characterization Experiment (Bates et al. 1998a); Atlantic aerosol—Second Aerosol Characterization Experiment (Raes et al. 2000); and recently heavy mixed aerosol in the Indian Ocean—Indian Ocean Experiment (Ramanathan et al. 2001); and southern Africa—Southern Africa Fire-Atmosphere Research Initiative] development of new satellite instrumentation (King et al. 1999), consistent analysis of historical satellite records (Jankowiak and Tanre 1992; Husar et al. 1997; Herman et al. 1997; Mishchenko et al.

++ Current affiliation: Naval Research Laboratory, Washington, D.C.

Corresponding author address: Alexander Smirnov, NASA Goddard Space Flight Center, Code 923, Greenbelt, MD 20771.
E-mail: asmirnov@aeronet.gsfc.nasa.gov

1999) and development of ground-based networks of radiometers for systematic and accurate long-term measurements (Holben et al 1998, 2001). The basic philosophy is that once these datasets are incorporated into aerosol and climate models in a consistent manner or used for their validation, we shall be able to better understand the role of aerosol in climate and improve the prediction of future changes (e.g., Kiehl and Briegleb 1993; Hansen et al. 1997). Without a comprehensive assessment of present aerosol concentrations and optical properties, we shall not be able to measure the change in the aerosol radiative forcing, and thus of the impact of changes of human activity on climate.

Field experiments provide the most comprehensive analysis of aerosol properties and their radiative impact [e.g., the comprehensive analysis of all aerosol impacts in the Indian Ocean by Ramanathan et al. (2001)] but they are limited in temporal and geographical extent. Satellites monitor the whole globe on a daily or weekly basis, and can generate long-term data sequences, but satellites derive aerosol information from the scattered light over varying terrain properties, and thus are limited in their information content and accuracy (e.g., Tanré et al. (1996). Remote sensing from ground-based sun–sky radiometers measures both the spectral attenuation of sunlight and the spectral-angular properties of scattered light—sky brightness. These measurements provide the most accurate and comprehensive long-term measurements of the optical properties of the ambient aerosol (Holben et al. 2001; Dubovik et al. 2002) in the entire atmospheric column, in specific instrumented locations.

In the current paper we analyze atmospheric aerosol optical properties using 2–5 yr of measurements by the Aerosol Robotic Network (AERONET) in five island locations in the Pacific and Atlantic Oceans. The AERONET solar attenuation and sky brightness measurements are used to derive the spectral optical thickness and size distribution of the column ambient aerosol. In contrast to in situ measurements, AERONET remote measurements do not characterize the aerosol chemical composition, but measure the optical properties of the aerosol, unaffected by sampling and drying processes inherent in in situ methods. The AERONET measurements are compared with a comprehensive survey of shipborne measurements published over the last 30 yr.

2. Historical overview

At the end of 1960s through the mid-1970s it became clear that our general knowledge of aerosol optical properties of the maritime atmosphere was very poor. Experimental data on aerosol optical properties above the oceans were scarce. Because of various reasons (data collection is very expensive, time and labor consuming, combined with instrumental and methodological difficulties) systematic experiments at sea were not conducted until the early 1980s. Since then significant progress has been made in the last 20 yr.

Table 1 summarizes the known published results of aerosol optical depth measurements in maritime and coastal areas. Unfortunately, numerous experiments were neither systematic nor extensive, employed only a few wavelengths, and measurement accuracy sometimes was unknown. However, the accumulated historical datasets can improve our understanding of aerosol optical depth spatial distributions, can become an important milestone in exploring the possibility of optical division into districts of the atmosphere above the oceans and establishing regional aerosol climatologies.

Data acquired over the Pacific Ocean indicate, generally, a more transparent atmosphere (small aerosol concentrations) as compared to the Atlantic Ocean, inland seas and coastal zones. Aerosol optical depth typically is low; however, long-range transport of dust from Asia during the spring months and global volcanic activity can increase the turbidity. Aerosol optical depth variability in remote oceanic areas is generally smaller than in the regions affected by continental sources. Spectral dependence of $\tau_a(\lambda)$ above the Pacific Ocean is more neutral than in coastal areas, owing to a large fraction of coarse-mode aerosol of sea origin (sea salt) in the size distribution.

Aerosol optical depth over the Atlantic Ocean shows large variability both temporally and spatially. It is greatly affected by the dust sources in Africa, pollutant sources in Europe and North America and biomass burning products in Africa and South America. Also, it can be noted that the spectral behavior of $\tau_a(\lambda)$ is more selective over the Atlantic than over the Pacific (higher Ångström parameter values correspond to generally higher extinction contributions from smaller particles). In the oceanic areas influenced by Saharan dust high turbidity [high $\tau_a(\lambda)$] corresponds to small values of Ångström parameter α, since in that case large particles of nonmaritime origin (dust) are dominant.

There is very little aerosol data for the Indian Ocean. Only recently an extensive field experiment measured the properties of aerosol in that region (Ramanathan et al. 1995). Aerosol optical depth is typical of background ocean values in the remote areas of the South Indian Ocean [south from the intertropical convergence zone (ITCZ)] (Matsubara 1983; Barteneva et al. 1991). The high $\tau_a(\lambda)$ in the Arabian Sea and areas close to Africa are associated with mineral dust, advected from Saudi Arabia, Iraq, southern Iran, and East Africa, and pollution aerosols from southwestern coast of India. The seasonality of the aerosol transport and relatively short period during ship cruises did not permit establishment of intraannual seasonal patterns in a majority of publications except for a paper by Moorthy and Satheesh (2000). Based on a 2-yr record they outlined the role of seasonally changing airmass type in causing a regular annual variation in spectral optical depths (τ_a ranges from 0.20 to 0.50 at a wavelength 500 nm). Eck et al.

TABLE 1. Summary of aerosol optical depth measurements in maritime and coastal areas.

Reference	Area	τ_a[a]	D[b]	Spectral range (nm)	No. of filters
Fischer (1967)	South Ocean	0.09	—[c]	500	1
	South Pacific Ocean	0.12	—		
	New Zealand coast	0.16	—		
Guttman (1968)	Marshall Islands	0.11	1	$450 \leq \lambda \leq 710$	7
Guschin (1970)	Indian and Atlantic Oceans	0.23	20	$370 \leq \lambda \leq 530$	2
Quenzel (1970)	Tropical Atlantic	0.23	3	$400 \leq \lambda \leq 1600$	8
Volz (1970)	Tropical Atlantic	0.18	17	$440 \leq \lambda \leq 1630$	4
Sandomirskiy et al. (1971)	Black Sea coast	0.27	—	$480 \leq \lambda \leq 2240$	6
Kuznetsov and Izhovkina (1973)	North Atlantic	0.04	—	$410 \leq \lambda \leq 550$	
Barteneva et al. (1974)	Tropical Atlantic	0.22	34	$350 \leq \lambda \leq 1010$	10
Burmistrova and Shubova (1974)	Tropical Pacific and Atlantic	0.18	26	550	1
Shifrin et al. (1975)	Indian Ocean	0.11	21	$330 \leq \lambda \leq 690$	5
Fraser (1976)	Atlantic Ocean–dust	0.50	1	$500 \leq \lambda \leq 1070$	2
Karimova (1976)	North Atlantic	0.08	5	$340 \leq \lambda \leq 630$	6
Emelyanov et al. (1978)	Atlantic Ocean	0.25	20	$440 \leq \lambda \leq 710$	4
Jaenicke and Schutz (1978)	Island Sal	0.38	—	$380 \leq \lambda \leq 500$	2
Adnashkin et al. (1979)	Tropical Atlantic	0.19	—	$350 \leq \lambda \leq 1010$	10
Tavartkiladze (1979)	Black Sea coast	0.28	—	$370 \leq \lambda \leq 820$	13
Wilson (1979)	San Diego	0.20	1	$400 \leq \lambda \leq 750$	10
	Gulf of Mexico	0.24	7		
	Bermuda	0.32	1		
Artemkin et al. (1980)	Atlantic Ocean	0.40	—	$400 \leq \lambda \leq 1060$	5
	South Ocean	0.16	—		
Shifrin et al. (1980b)	Black Sea coast	0.16	2	$340 \leq \lambda \leq 960$	9
Shifrin et al. (1980a)	Baltic Sea coast	0.20	2	$380 \leq \lambda \leq 720$	5
Viollier et al. (1980)	Azores	0.41	182	$400 \leq \lambda \leq 1000$	
Hogan (1981)	South Pacific Ocean	0.17	7	$520 \leq \lambda \leq 620$	2
	Ross Sea	0.14	5		
Lukyanchikova and Govorushkin (1981)	North Atlantic	0.10	11	$370 \leq \lambda \leq 570$	4
Sakunov et al. (1981)	Beaufort Sea	0.07	8	$350 \leq \lambda \leq 1000$	10
Tomasi and Prodi (1982)	Indian Ocean	0.27	16	$500 \leq \lambda \leq 880$	2
	Coast of Somalia	0.36	24		
Yershov et al. (1982)	Central Atlantic	0.17	16	$380 \leq \lambda \leq 1016$	11
Afonin (1983)	Black Sea	0.30	—	$400 \leq \lambda \leq 750$	8
	Mediterranean Sea	0.39	—		
	Atlantic Ocean	0.05	—		
	Coast of Guinea	0.90	—		
Artemkin and Krivoshein (1983b)	North Atlantic	0.14	—	$430 \leq \lambda \leq 850$	5
	Central Atlantic	0.09	—		
Artemkin and Krivoshein (1983a)	Baltic and North Seas	0.28	—	$430 \leq \lambda \leq 850$	5
	West African coast	0.37	—		5
Gashko and Shifrin (1983)	Pacific Ocean	0.14	23	$370 \leq \lambda \leq 720$	7
Eerme (1983)	Baltic Sea	0.17	9	$450 \leq \lambda \leq 710$	7
Matsubara et al. (1983)	East Indian Ocean	0.09	7	$370 \leq \lambda \leq 860$	5
	South Indian Ocean	0.04	4		
Shaw (1983)	Central Pacific Ocean	0.10	—	$410 \leq \lambda \leq 1000$	9
Villevalde et al. (1984)	Mediterranean Sea	0.50	10	$380 \leq \lambda \leq 560$	9
Shifrin et al. (1985)	Black Sea coast	0.18	15	$440 \leq \lambda \leq 1030$	6
	Baltic and North Sea	0.17	2		
	Mediterranean Sea	0.25	5		
	Red Sea	0.18	13		
	South China Sea	0.20	2		
	Indian Ocean	0.20	5		
	Atlantic Ocean	0.30	2		
Platt and Patterson (1986)	Coast of Tasmania, summer	0.12	—	500	1
	Coast of Tasmania, winter	0.08	—		
Yershov and Smirnov (1986)	Black Sea coast	0.23	13	$440 \leq \lambda \leq 1030$	7
von Hoyningen-Huene and Raabe (1987)	Atlantic Ocean	0.23	3	$350 \leq \lambda \leq 1055$	20
Deuze et al. (1988)	Mediterranean Sea	0.68	4	$450 \leq \lambda \leq 2200$	7
Volgin et al. (1988)	Mediterranean Sea	0.20	27	$440 \leq \lambda \leq 1030$	7
	Pacific Ocean	0.07	33		
	Atlantic Ocean–dust	0.42	9		
Weller and Leiterer (1988)	Baltic Sea	0.18	—	$380 \leq \lambda \leq 1100$	40
	Atlantic Ocean	0.12	—		
	Indian Ocean	0.05	—		
	Java Sea	0.10	1		
	South China Sea	0.08	1		

TABLE 1. (*Continued*)

Reference	Area	τ_a[a]	D[b]	Spectral range (nm)	No. of filters
Zibordi and Maracci (1988)	Mediterranean Sea	0.60	4	$500 \leq \lambda \leq 700$	
Villevalde et al. (1989)	Baltic Sea	0.23	5	$380 \leq \lambda \leq 1020$	12
	North Atlantic	0.17	5		
Haggerty et al. (1990)	Mediterranean Sea	0.09	4	502	1
Hoppel et al. (1990)	Tropical Atlantic	0.15	10	$440 \leq \lambda \leq 880$	4
Reddy et al. (1990)	Bermuda	0.22	—	$380 \leq \lambda \leq 500$	2
	Canary Islands (without dust)	0.09	—	$380 \leq \lambda \leq 500$	2
	Canary Islands (with dust)	0.37	—		
	North American air	0.50	7	$380 \leq \lambda \leq 780$	4
	Atlantic air	0.15	6		
	Saharan air	0.38	2		
Smirnov and Gulyaev (1990)	Central Atlantic	0.18	11	$506 \leq \lambda \leq 1030$	6
Yershov et al. (1990)	Mediterranean Sea	0.21	19	$440 \leq \lambda \leq 1030$	7
	Central Atlantic	0.12	15		
Barteneva et al. (1991)	North Atlantic, 1982	0.17	—	$350 \leq \lambda \leq 1010$	9
	North Atlantic, 1983	0.20	—		
	Subtropical Atlantic	0.07	—		
	Carribean Sea	0.10	—		
	Tropical Atlantic	0.10	—		
	Red Sea	0.33	—		
	Pacific Ocean	0.21	—	$350 \leq \lambda \leq 1010$	10
	Indian Ocean	0.11	—		
	South Indian Ocean	0.07	—		
	South Ocean, 1982	0.09	—		
	South Ocean, 1987	0.04	—		
Moorthy et al. (1991)	India, west coast, summer	0.50	—	$400 \leq \lambda \leq 1025$	9
	India, west coast, winter	0.25	—		
Wolgin et al. (1991)	North Atlantic	0.11	9	$460 \leq \lambda \leq 1640$	9
Ignatov et al. (1993)	Canary Islands	0.19	—	$450 \leq \lambda \leq 1060$	6
	Central Atlantic	0.15	—		
Korotaev et al. (1993)	Europe	0.22	7	$480 \leq \lambda \leq 1060$	6
	Nord	0.07	9		
	Bermuda	0.08	10		
	Atlantic Ocean–dust	0.37	10		
	Atlantic Ocean–dust	0.29	14		
	Canary Islands	0.06	9		
	Mediterranean Sea	0.06	6		
Clarke and Porter (1994)	Pacific Ocean, 32°N, 170°W	0.23	—	550	
	Pacific Ocean, 22°N, 170°W	0.13	—		
	Pacific Ocean, 17°N, 170°W	0.24	—		
	Pacific Ocean, 8°N, 170°W	0.10	—		
	Pacific Ocean, 0°N, 170°W	0.07	—		
	Pacific Ocean, 5°S, 170°W	0.05	—		
Hayassaka et al. (1994)	Pacific Ocean, 30°N	0.12	—	$368 \leq \lambda \leq 778$	4
	Pacific Ocean, 25°N	0.08	—		
	Pacific Ocean, 17°N	0.11	—		
	Pacific Ocean, 2°S	0.12	—		
	Pacific Ocean, 8°S	0.07	—		
	Pacific Ocean, 25°S	0.06	—		
	Pacific Ocean, 38°S	0.08	—		
Villevalde et al. (1994)	North Atlantic	0.11	6	$490 \leq \lambda \leq 1640$	8
	Pacific Ocean	0.13	30	$460 \leq \lambda \leq 1640$	10
von Hoyningen-Huene and Wendisch (1994)	Baltic Sea coast, Maritime air	0.11	—	$350 \leq \lambda \leq 1100$	
	Continental polar air	0.21	—		40
Sakerin et al. (1995)	Europe	0.19	73	$370 \leq \lambda \leq 1060$	12
	Canary Islands	0.14			
	Atlantic Ocean–dust	0.49			
Smirnov et al. (1995a)	North Atlantic	0.13	6	$460 \leq \lambda \leq 1640$	6
Smirnov et al. (1995b)	Mediterranean Sea, winter	0.05	3	$440 \leq \lambda \leq 1030$	6
	Mediterranean Sea, fall	0.21	7		
	Black Sea	0.33	5		
	Central Atlantic	0.14	8		
	Subtropical Atlantic, winter	0.07	12		
	Subtropical Atlantic, fall	0.24	12		
	West African coast, winter	0.08	3		
	West African coast, fall	0.39	3		

TABLE 1. (*Continued*)

Reference	Area	τ_a[a]	D[b]	Spectral range (nm)	No. of filters
Quinn (1995, unpublished data)	Pacific Ocean	0.08	32	$380 \leq \lambda \leq 865$	4
Kusnierczyk-Michulec and Darecki (1996)	Baltic Sea	0.25	19	$410 \leq \lambda \leq 865$	6
Sakerin and Kabanov (1997)	Central Atlantic	0.06	25	$370 \leq \lambda \leq 4000$	13
	North Sea, English Channel	0.12			
Moorthy et al. (1997)	Indian Ocean	0.19	20	$380 \leq \lambda \leq 1025$	10
Moulin et al. (1997)	Coast of Corsica	0.11	12	$450 \leq \lambda \leq 940$	5
	Tropical Atlantic	0.46	15		
	Sal Island, 1991	0.21	8		
	Sal Island, 1992	0.50	4		
Satheesh et al. (1998)	Indian Ocean, Arabian Sea	—	29	$380 \leq \lambda \leq 1025$	10
Smirnov et al. (1998)	Canary Islands	0.16	23	$340 \leq \lambda \leq 1020$	8
Kusnierczyk-Michulec et al. (1999)	Baltic Sea	0.21	27	$410 \leq \lambda \leq 865$	6
Masuda et al. (1999)	Pacific Ocean	0.08	4	$440 \leq \lambda \leq 870$	6
	Sea of Japan	0.16	2		
Murayama et al. (1999)	Coast of Tokyo Bay	—	4	$368 \leq \lambda \leq 778$	4
Satheesh et al. (1999)	Maldives, Indian Ocean	0.17	33	$340 \leq \lambda \leq 1020$	8
Moorthy and Saha (2000)	Indian Ocean, Arabian Sea	—	96	$380 \leq \lambda \leq 1025$	10
Moorthy and Satheesh (2000)	Minicoy (Arabian Sea)	0.29	272	$380 \leq \lambda \leq 1025$	10
Smirnov et al. (2000a)	Atlantic Ocean	0.18	9	$340 \leq \lambda \leq 1020$	8
	Bermuda	0.17	23		
Livingston et al. (2000)	Atlantic Ocean, Canary	0.14	9	$380 \leq \lambda \leq 1020$	6
Porter et al. (2001)	Pacific (north of Hawaii)	0.08	3	$380 \leq \lambda \leq 1020$	7
Voss et al. (2001)	North Atlantic marine air	0.09	6	$380 \leq \lambda \leq 870$	6
	African dust	0.28	3		
	Biomass burning	0.33	3		
	South Atlantic tropical air	0.10	6		
	South Atlantic temperate air	0.10	3		

[a] τ_a is the mean value of aerosol optical depth at a wavelength 550 nm.
[b] D is the number of measurement days.
[c] Three centered dots indicate that no information is available.

(2001) presented an analysis of the column-integrated optical properties over the Maldives during the northeast monsoon for 1998–2000. Large interannual variability was observed during the NE monsoon months of January through April. Spectral variation of optical depth also exhibited interannual variability, associated not only with the anthropogenic plumes but also as a result of variability in dust transport from arid and semiarid regions.

Measurements made in inland seas (Mediterranean, Red, Black, Baltic, North, South China) and coastal zones yielded generally higher values of optical depth than over open oceanic areas. Optical conditions are greatly influenced by continental aerosols including dust in the Mediterranean and Red Seas. Strong wavelength dependence of $\tau_a(\lambda)$ for coastal areas and inland seas is indicative of a large number of small particles of continental origin in a total column size distribution. Comparison of aerosol optical depths obtained over the Mediterranean Sea by various research groups indicated substantial seasonal difference. Since the majority of measurements were made during the June–September period we cannot form definitive conclusions on the seasonal behavior of τ_a. Nevertheless, the more apparent changes of optical properties from summer to winter can be delineated.

Physical and chemical properties of maritime aerosols are important for various applications. They play an important role in a number of atmospheric processes and affect the performance of various electrical and optical systems. In the last few decades a number of outstanding reviews on maritime aerosol properties have been published (e.g., Junge 1972; Blanchard and Woodcock 1980; Podzimek 1980; Fitzgerald 1991; de Leeuw 1991). Original results on particle concentrations, size distributions, composition, and sources of aerosol presented in a historical perspective give a full-scale picture of the state-of-the-art knowledge of the maritime aerosol properties.

We do not intend to present an up-to-date review of the particle size distributions over the oceans. However, in Table 2 we summarize the more recent publications on the in situ measurements of aerosol size distributions. Only those publications that presented fitting parameters for size distributions have been considered. Therefore, some publications are absent from Table 2, for example, an outstanding paper by Hoppel et al. (1990).

Table 2 presents parameters of the lognormal volume size distributions (Whitby 1978). For each mode the lognormal distribution is defined as

TABLE 2. Parameters of aerosol size distributions over the oceans.

Reference	Area	Height (m)	Date	Air mass type	Fraction	R_V (μm)	σ	V (μm^3 cm^{-3})
Shettle and Fenn (1979)				Continental	Fine (dry)	0.19	0.81	
				Oceanic	Coarse (dry)	2.03	0.92	
Gathman (1983)				Maritime	Fine (RH = 80%)	0.14	0.71	
					Coarse (RH = 80%)	1.09	0.71	
					Giant (RH = 80%)	9.07	0.71	
Horvath et al. (1990)	Near Bermuda	250	6 Apr 1985		Coarse (ambient)	2.56	0.525	95.4
	Near Bermuda	1500	6 Apr 1985		Coarse (ambient)	1.65	0.756	1.17
	U.S. east coast, Virginia	100	27 Feb 1985		Coarse (ambient)	4.19	0.742	18.8
	U.S. east coast, Virginia	1500	27 Feb 1985		Coarse (ambient)	3.83	0.732	7.0
Patterson et al. (1980) as presented by Horvath et al. (1990)	Pacific Ocean				Coarse (ambient)	1.29	0.457	
Jennings and O'Dowd (1990)	Mace Head	20	1 Jun 1988		Fine (ambient)	0.10	0.30	0.89
					Coarse (ambient)	1.40	0.73	20.04
Kim et al. (1990)	Atlantic Ocean off Bermuda	150	Jul 1988		Fine (ambient)	0.11	0.33	0.74
					Large (ambient)	0.74	0.46	1.13
					Giant (ambient)	2.96	0.44	20.90
	Atlantic Ocean off Bermuda	2570	Jul 1988		Fine (ambient)	0.11	0.52	0.13
					Large (ambient)	0.71	0.52	0.30
					Giant (ambient)	2.78	0.58	2.00
	U.S. east coast, North Carolina	150	Jul 1988		Fine (ambient)	0.12	0.37	3.63
					Large (ambient)	0.81	0.46	3.63
					Giant (ambient)	3.63	0.50	132.3
	U.S. east coast, North Carolina	2570	Jul 1988		Fine (ambient)	0.13	0.46	2.11
					Large (ambient)	0.70	0.45	0.63
					Giant (ambient)	3.16	0.59	5.94
O'Dowd et al. (1993)	Northeast Atlantic in the vicinity of Faeroe Island and Iceland	18	Oct–Nov 1989	Maritime	Accumulation (dry)	0.11	0.315	0.15
				Modified Maritime	Accumulation (dry)	0.14	0.301	2.19
				Arctic	Accumulation (dry)	0.13	0.328	0.17
				Continental Maritime	Accumulation (dry)	0.12	0.332	2.55
Pueschel et al. (1994)	Southern Pacific Ocean	10 000	Nov 1989		Fine (ambient)	0.10	0.41	0.038
					Coarse (ambient)	0.28	0.34	0.034
Kim et al. (1995)	Atlantic Ocean off the Azores	10	12 Jun 1992		Fine (dry)	0.10	0.39	0.89
					Coarse (dry)	0.50	0.65	1.17
	Atlantic Ocean off the Azores	10	19 Jun 1992		Fine (RH = 77%)	0.14	0.47	1.88
					Coarse (RH = 77%)	0.40	0.75	4.05
	Atlantic Ocean off the Azores	10	24 Jun 1992		Fine (RH = 71%)	0.11	0.26	0.72
					Coarse (RH = 71%)	0.35	0.59	3.67
Gras (1995)	Cape Grim		Jan 1991–Jun 1992	Autumn	CN (dry)	0.014	0.38	0.001
					CNN (dry)	0.10	0.37	0.16
					Large (dry)	0.78	0.61	2.38
				Winter	CN (dry)	0.010	0.30	0.000
					CNN (dry)	0.19	0.49	0.35
					Large (dry)	0.77	0.57	3.90
				Spring	CN (dry)	0.013	0.38	0.001
					CNN (dry)	0.14	0.45	0.25
					Large (dry)	0.62	0.54	1.90
				Summer	CN (dry)	0.016	0.38	0.003
					CNN (dry)	0.11	0.37	0.34
					Large (dry)	0.89	0.60	4.51
Quinn et al. (1995)	U.S. west coast Cheeka Peak	480	Apr–May 1991		Aitken (dry)	0.04	0.41	0.04
					Accumulation (dry)	0.13	0.34	0.51
					Coarse (dry)	0.98	0.69	2.65
	Pacific Ocean	18	Feb–Mar 1992		Aitken (dry)	0.03	0.34	0.01
					Accumulation (dry)	0.13	0.34	0.68
					Coarse (dry)	1.22	0.59	8.99

TABLE 2. (*Continued*)

Reference	Area	Height (m)	Date	Air mass type	Fraction	R_v (μm)	σ	V (μm^3 cm^{-3})
Quinn et al. (1996)	Pacific Ocean	18	Mar–May 1993	Maritime	Accumulation (dry)	0.10	0.27	0.14
					Coarse (dry)	1.36	0.60	7.34
	Pacific Ocean	18	Mar–May 1993	Continental	Accumulation (dry)	0.15	0.29	0.49
					Coarse (dry)	1.22	0.60	4.82
Porter and Clarke (1997)	Pacific and Indian Oceans	20		Maritime PC4	Fine (dry)	0.135	0.48	
					Coarse (dry)	3.45	0.84	
O'Dowd et al. (1997)	Northeast Atlantic	18	Oct–Nov 1989		Film drop mode (dry)	0.34	0.64	
					Jet drop mode (dry)	4.17	0.69	
Jennings et al. (1997)	Mace Head	20	Nov 1993–Aug 1994	Winter marine	Accumulation (ambient)	0.2–0.25	0.69	
					Coarse (ambient)	2.0	0.92	
				Summer marine	Accumulation (ambient)	0.2–0.25	0.69	
					Coarse (ambient)	2.5	0.69	
Hess et al. (1998)					Water-soluble (dry)	0.15	0.81	
					Accumulation (dry)	0.94	0.71	
					Coarse (dry)	7.90	0.71	
Brechtel et al. (1998)	Macquarie Island, Southern Ocean		Nov–Dec 1995	Maritime	Aitken (dry)	0.02	0.34	0.012
					Accumulation (dry)	0.11	0.46	0.27
Bates et al. (1998b)	Southern Ocean	18	Nov–Dec 1995	Maritime	Ultrafine (dry)	0.01	0.37	0.001
					Aitken (dry)	0.02	0.34	0.007
					Accumulation (dry)	0.08	0.34	0.09
					Coarse (dry)	1.19	0.70	11.44
				Continental	Ultrafine (dry)	0.01	0.35	0.003
					Aitken (dry)	0.03	0.41	0.04
					Accumulation (dry)	0.08	0.28	0.12
					Coarse (dry)	1.33	0.73	20.03
Bates et al. (2000)	Atlantic Ocean	10	Jun–Jul 1997	Atlantic flow	Nucleation (dry)	0.008	0.17	0.000
					Aitken (dry)	0.027	0.36	0.011
					Accumulation (dry)	0.127	0.36	0.515
				Arctic flow	Nucleation (dry)	0.008	0.20	0.000
					Aitken (dry)	0.025	0.32	0.016
					Accumulation (dry)	0.123	0.35	0.492
Quinn et al. (2001)	Atlantic Ocean	10	Jan–Feb 2000	North America	Fine (RH = 55%)	0.14	0.34	3.70
					Coarse I (RH = 55%)	0.57	0.59	6.18
					Coarse II (RH = 55%)	1.75	0.47	25.05
				North Atlantic marine	Fine (RH = 55%)	0.12	0.34	0.310
					Coarse I (RH = 55%)	1.04	0.74	7.37
					Coarse II (RH = 55%)	1.79	0.53	24.35
				African dust	Fine (RH = 55%)	0.10	0.34	0.349
					Coarse I (RH = 55%)	0.68	0.64	9.22
					Coarse II (RH = 55%)	1.31	0.47	32.05
				Dust and biomass burning	Fine (RH = 55%)	0.18	0.53	2.69
					Coarse I (RH = 55%)	1.13	0.53	25.44
				Biomass burning	Fine (RH = 55%)	0.16	0.41	2.54
					Coarse I (RH = 55%)	1.19	0.53	5.87
				South Atlantic tropical marine	Fine (RH = 55%)	0.18	0.41	1.03
					Coarse I (RH = 55%)	1.59	0.64	11.61
				South Atlantic temperate marine	Fine (RH = 55%)	0.13	0.26	1.04
					Coarse I (RH = 55%)	2.08	0.74	27.92
Reid et al. (2001)	Outer Banks, North Carolina	30–100	Feb–Mar 1999		Coarse (ambient)	4.5	0.6–0.8	

$$\frac{dV}{d\ \ln R} = \frac{V_0}{\sigma\sqrt{2\pi}} \exp\left[-\frac{1}{2}\left(\frac{\ln(R/R_v)}{\sigma}\right)^2\right],$$

where $dV/d\ \ln R$ is the volume size distribution, the volume concentration V_0 is the volume of particles, R is the particle radius, R_v is the volume geometric mean radius, σ is the geometric standard deviation.

Comparison of aerosol size distribution parameters

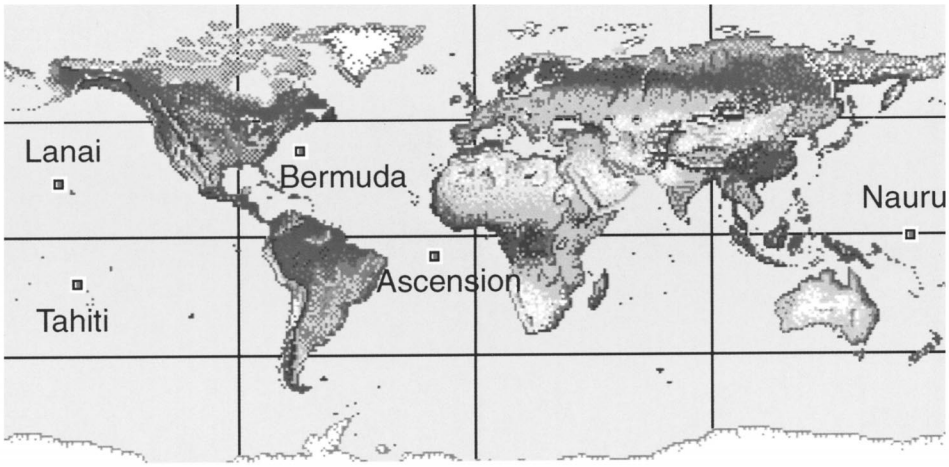

FIG. 1. Map of the five AERONET sites used in the study.

presented in Table 2 showed a good agreement for the fine-mode aerosol. Parameter R_v ranges below 0.10 μm–0.15 μm. The position of the fine-mode maximum is not dependent on measurement area and particular instrumentation. However, the results obtained for the coarse-mode aerosols indicated large variations in R_v and substantial differences from publication to publication. The cause of such disparity could be associated with the instrumental uncertainties and changing environmental conditions, that is, wind speed, wind-speed history, relative-humidity history, precipitation, etc. (Gathman 1983; Hoppel et al. 1990).

3. Data collection

Aerosol optical properties were derived from direct sun and sky radiation measurements performed at the operational AERONET sites in the Pacific (Nauru, Lanai, Tahiti) and in the Atlantic (Bermuda, Ascension Island; Fig. 1).

The island of Nauru (0°30′S, 166°54′E) is situated in the tropical western Pacific Ocean. The island is very small with a total land area ~25 km^2. It lies ~40 km south of the equator and the nearest neighbor island is 300 km away. Nauru is a good example of an equatorial oceanic site and was chosen by the Atmospheric Radiation Measurement Program to set up a Cloud and Radiation Testbed site (Mather et al. 1998).

The island of Lanai (20°49′N, 156°59′W) is situated in the tropical Pacific Ocean. It is a part of the Hawaiian Islands. Lanai has a total land area of ~365 km^2, and is more than 3500 km away from the nearest continental landmass (California coast). Therefore, air that reaches it, regardless of source, spends enough time over the ocean to be considered ''truly maritime.'' Long-distance high-altitude dust transport from Asia is an only exception. Because of the shelter provided by the surrounding islands, Lanai receives very little rain and is not known for large waves (Price 1983).

Tahiti is the largest island in French Polynesia. It is situated in the eastern South Pacific at 17°32′S, 149°34′W. Tahiti has a total land area of ~1000 km^2 and is 5400 km away from the nearest continent (Australia). The tropical climate has two distinct seasons here, wet season, between November and April, and dry season, between May and October.

Bermuda is an archipelago of seven islands situated in the western North Atlantic Ocean, approximately 1050 km from Cape Hatteras (North Carolina, U.S. east coast). Climate on Bermuda is subtropical with no wet season. Air that reaches Bermuda cannot always be considered truly maritime. One can observe three different optical conditions associated with various aerosol sources, which are defined in terms of generalized source trajectories: pure Atlantic air, air from North America, and Saharan dust (Reddy et al. 1990; Smirnov et al. 2000a). A sun photometer was located at the Bermuda Biological Station (32°22′N, 64°41′W).

The small island of Ascension is situated in the South Atlantic (07°56′S, 14°22′W) and covers an area of ~80 km^2. Ascension is a rocky peak of purely volcanic origin. The climate is tropical. Dust and biomass burning aerosols from Africa reach Ascension Island. Although such occurrences are sporadic they affect the optical properties over the island.

All of the measurements reported in this paper were made with the automatic sun and sky scanning radiometers CIMEL. Three of the instruments deployed (Lanai, Tahiti, and Ascension) were CIMEL radiometers belonging to the Sensor Intercomparison and Merger for Biological and Interdisciplinary Oceanic Studies project (McClain and Fargion 1999). Four instruments (Nauru, Lanai, Tahiti and Ascension) were reengineered. The reengineering included a number of modifications

to ''harden'' the sun–sky radiometer for deployments in corrosive marine environments.

The CIMEL radiometers made measurements of the direct sun and diffuse sky radiances within the spectral range 340–1020 nm and 440–1020 nm, respectively (Holben et al. 1998). The direct sun measurements are acquired in eight spectral channels at 340, 380, 440, 500, 670, 870, 940, and 1020 nm (nominal wavelengths). Seven of the eight bands are used to acquire aerosol optical depth data. The eighth band at 940 nm is used to estimate total precipitable water content. The bandwidths of the ion-assisted deposition interference filters employed in the CIMEL radiometer vary from 2–4 nm (UV channels) to 10 nm for visible and near-infrared channels.

Holben et al. (1998) and Eck et al. (1999) presented careful assessments of the overall uncertainty in computed τ_a due to calibration uncertainty, lack of surface pressure data and actual ozone column amount. Typically, the total uncertainty in $\tau_a(\lambda)$ for a field instrument is $\sim\Delta\tau_a = \pm 0.01$ to ± 0.02, and is spectrally dependent with the higher errors (± 0.02) in the UV spectral range. Schmid et al. (1999) showed that discrepancies between aerosol optical depths measured by a CIMEL radiometer and four other radiometers in field experimental conditions were within 0.015 (rms). The details of the water vapor content (WVC) retrieval procedure and the types of errors involved can be found in Schmid et al. (2001).

An automatized and computerized cloud-screening algorithm (Smirnov et al. 2000b) was applied to the direct sun measurements.

The sky radiance almucantar measurements are acquired in four spectral channels at 440, 670, 870, and 1020 nm. For each solar zenith angle sky radiances are taken at 28 azimuth angles within the relative azimuth angle range (from the sun) of 2°–180° (Holben et al. 1998). A flexible inversion algorithm for retrieval of aerosol optical properties, developed by Dubovik and King (2000), was used for retrieving aerosol volume size distributions over a range of radii from 0.05 to 15 μm together with spectrally dependent complex refractive index and single scattering albedos from spectral sun and sky radiance data. An inversion strategy, details of the algorithm development and the methodological aspects of a detailed statistical optimization of the influence of noise in the inversion procedure are discussed in depth in (Dubovik and King 2000).

The accuracy of the retrieved aerosol particle size distributions and single scattering albedos (SSA) has been studied in detail by Dubovik et al. (2000). Retrieval errors in $dV/d\ \ln R$ typically do not exceed 15% for water-soluble aerosol type for each particle radius within the 0.1–7-μm range. The errors for very small particles ($r \sim 0.05$–0.1 μm) and very large particles ($r \sim 7$–15 μm) may be as large as 15%–100% (for each particle radius bin). However, no significant shifts in the positions of mode radii or changes in the shape of size distributions are expected. Single scattering albedos (SSAs) are expected to have an uncertainty of 0.05–0.07 for water soluble aerosol type and when $\tau_a(440\ \text{nm}) < 0.20$ (Dubovik et al. 2000).

For simplicity we will characterize the atmospheric aerosol optical properties by two parameters: $\tau_a(500$ nm), which is the aerosol optical depth at a wavelength 500 nm, and the Ångström parameter α, derived from a multispectral log–linear fit to the classical equation $\tau_a \sim \lambda^{-\alpha}$ (based on 4 wavelengths in the range 440–870 nm). Although not all optical depth spectra are well-represented by an Ångström fit (see e.g., Knestrick et al. 1962; King and Byrne 1976; Kaufman 1993; Villevalde et al. 1994; Eck et al. 1999; O'Neill et al. 2001), α can still be considered as a first-order parameter indicative of the general size distribution and the relative dominance of fine- versus coarse-mode particles. It is noted that for bimodal size distributions with a significant coarse-mode and coarse-mode-dominated size distributions the spectral curvature of $\ln\tau_a$ versus $\ln\lambda$ is very small (Eck et al. 1999).

4. Results

a. Aerosol optical depth statistics

The significant number of the data sources considered in Table 1 gave an opportunity to evaluate the real variability of aerosol optical depth and Ångström parameter for various regions. One can observe that the largest optical variability occurs in the Atlantic Ocean. This high degree of variability is largely attributable to the diverse contributions of a variety of continental aerosol sources (urban–industrial, dust, and biomass burning). The enrichment of maritime air by ''stationary'' and ''fresh'' sea-spray aerosol components (Gathman 1983) is an additional source of variability. We estimate that the combination of five datasets considered in the current study (three over the Pacific and two over the Atlantic) is sufficient for the characterization of the background optical conditions over the oceans in the tropical and subtropical regions.

Table 3 summarizes measurements of aerosol optical depth in oceanic areas for which analyses have been performed in the current study. One can observe indications of differences between Pacific and Atlantic sites in terms of the aerosol optical depth value as well as the Ångström parameter. As would be expected, optical depth is higher over the Atlantic sites (mixed maritime aerosol type) than over the Pacific. The smaller mean α value over Nauru as compared to the other sites may be attributed, in the first instance, to the smallest island area and to different degree of sea-spray production and deposition.

The mean $\tau_a(500$ nm) values of 0.07–0.08 for the Pacific sites are close to the results presented by Masuda et al. (1999), Quinn (1995, unpublished data), Clarke and Porter (1994), Volgin et al. (1988), and Shaw (1983) (see Table 1). Standard deviation (σ) of 0.02–0.03 is an

TABLE 3. Statistical characteristics of aerosol optical depth and Ångström parameter α.

Site	Time period	N[a]	Aerosol type	τ_a[b]	σ[c]	α[d]	σ_α[e]	τ_{am}[b]	α_m[d]
Lanai, Pacific Ocean	Nov 1995–Apr 2000	722	Maritime	0.07	0.05	0.76	0.37	0.06	0.70
Nauru, Pacific Ocean	Jun 1999–Apr 2000	276	Maritime	0.08	0.03	0.43	0.35	0.06	0.30
Tahiti, Pacific Ocean	Jul 1999–May 2000	234	Maritime	0.07	0.02	0.74	0.27	0.06	0.70
Bermuda, Atlantic Ocean	Mar 1996–Dec 1999	590	Mixed maritime	0.14	0.09	0.93	0.41	0.09	0.90
Ascension, Atlantic Ocean	Nov 1998–Jun 2000	338	Mixed maritime	0.13	0.07	0.62	0.30	0.11	0.70

[a] N, number of analyzed days.
[b] τ_a and τ_{am} mean and mode values of aerosol optical depth at a wavelength 500 nm.
[c] σ standard deviation of the aerosol optical depth.
[d] α and α_m mean and mode values of the Ångström parameter.
[e] σ_α, standard deviation of the Ångström parameter.

indicative of small natural variability of aerosol optical depth in this region. The value of $\sigma = 0.02$ was reported by Volgin et al. (1988) based on a series of 48 measurements in the Pacific. The mean α value of 0.43 at Nauru is close to the values of 0.56 and 0.45 reported by Villevalde et al. (1994) and Volgin et al. (1988) for the Pacific.

The mean τ_a(500 nm) values of 0.13–0.14 for the two AERONET Atlantic sites differ almost by a factor of 2 from the Pacific AERONET data. This value agrees with the results reported by Reddy et al. (1990), Hoppel et al. (1990), Ignatov et al. (1993), Korotaev et al. (1993), and Smirnov et al. (1995b, 2000a) (see Table 1) within one standard deviation. The larger variability of optical properties over Bermuda and Ascension caused standard deviation to increase by a factor of 2, at least, compared to the clean remote maritime conditions in the Pacific. The mean value of the Ångström parameter at Bermuda (0.93) is higher than over the Pacific sites, but very close to the values reported by Hoppel et al. (1990), Reddy et al. (1990), Villevalde et al. (1994), and Smirnov et al. (1995a,b) for the Atlantic.

Figure 2a illustrates the daily averaged aerosol optical depth at 500 nm for Nauru. Daily average values show small day-to-day variation. Computed standard deviations of daily τ_a(500 nm) range from below 0.01 to 0.05 (Fig. 2b). The Ångström parameter α showed that coarse particles (small α) almost always influence atmospheric aerosol optical properties above Nauru (Fig. 2c). The values of α which are typically less than 0.5 indicate the presence of coarse-mode sea-salt aerosol. Mean daily values of the WVC are, generally, between 3 and 6 cm of precipitable water (Fig. 2d) with no intraannual signature over the data interval.

Daily mean values of τ_a(500 nm) over Lanai (Fig. 3a) show the spring seasonal peaks. The seasonal variation of the monthly average aerosol optical depth showed maximum in the spring season months (March, April, and May) (Holben et al. 2001). This seasonal peak in spring is due to the long-ranged transport of Asian aerosols (Shaw 1980; Bodhaine et al. 1981). Perry et al. (1999) suggested that the long-range transport of biomass burning aerosols from Mexico and Central America could affect optical conditions over Hawaii. Daily variations are also due in part to variation in the production and transport of volcanic aerosols from the active volcanoes on the island of Hawaii. Computed standard deviations of daily τ_a(500 nm) generally are less than 0.04 (Fig. 3b). The Ångström parameter α showed larger variability than over Nauru (Fig. 3c). Daily average water vapor contents (Fig. 3d) range from less than 2 cm to 5 cm and exhibit some seasonality with higher values in the summer.

Elimination of the spring (March, April, May) data (influenced by possible dust and volcano aerosol contamination) from the Lanai dataset did not change mode values of the optical parameters. Further analysis performed by Kaufman et al. (2001) derived optical properties of the baseline aerosol, that are very close to the results reported in the current study.

Daily averages of τ_a(500 nm) over Tahiti and its standard deviations are shown in Figs. 4a and 4b, respectively. Day-to-day variability is low, indicating a relative stability of optical properties. In the majority of cases the computed standard deviations of daily τ_a(500 nm) range below 0.03 (Fig. 4b). The Ångström parameter α (Fig. 4c) showed smaller variability than over Lanai and Nauru. The daily average values of the water vapor content (Fig. 4d) show higher values in the summertime (December, January, February). This is consistent with the general synoptic pattern for the area.

Figure 5a presents the daily averaged aerosol optical depth at 500 nm for the measurement period over Bermuda. The aerosol optical depth for this site is higher in the summertime (see also Holben et al. 2001), which is associated with dust transport from the Sahara–Sahel regions and urban–industrial aerosol from North America (Reddy et al. 1990; Smirnov et al. 2000a). Standard deviations of daily τ_a(500 nm) range generally below 0.03, however, occasionally can far exceed this value (Fig. 5b). Daily average values of α show significant variability and large day to day variation (Fig. 5c). WVC exhibits a pronounced seasonal pattern with a maximum in July and August.

As previously mentioned dust and biomass burning aerosols from Africa can reach Ascension Island. However, the optical depth range and daily standard deviations (Figs. 6a and 6b) are smaller than over Bermuda.

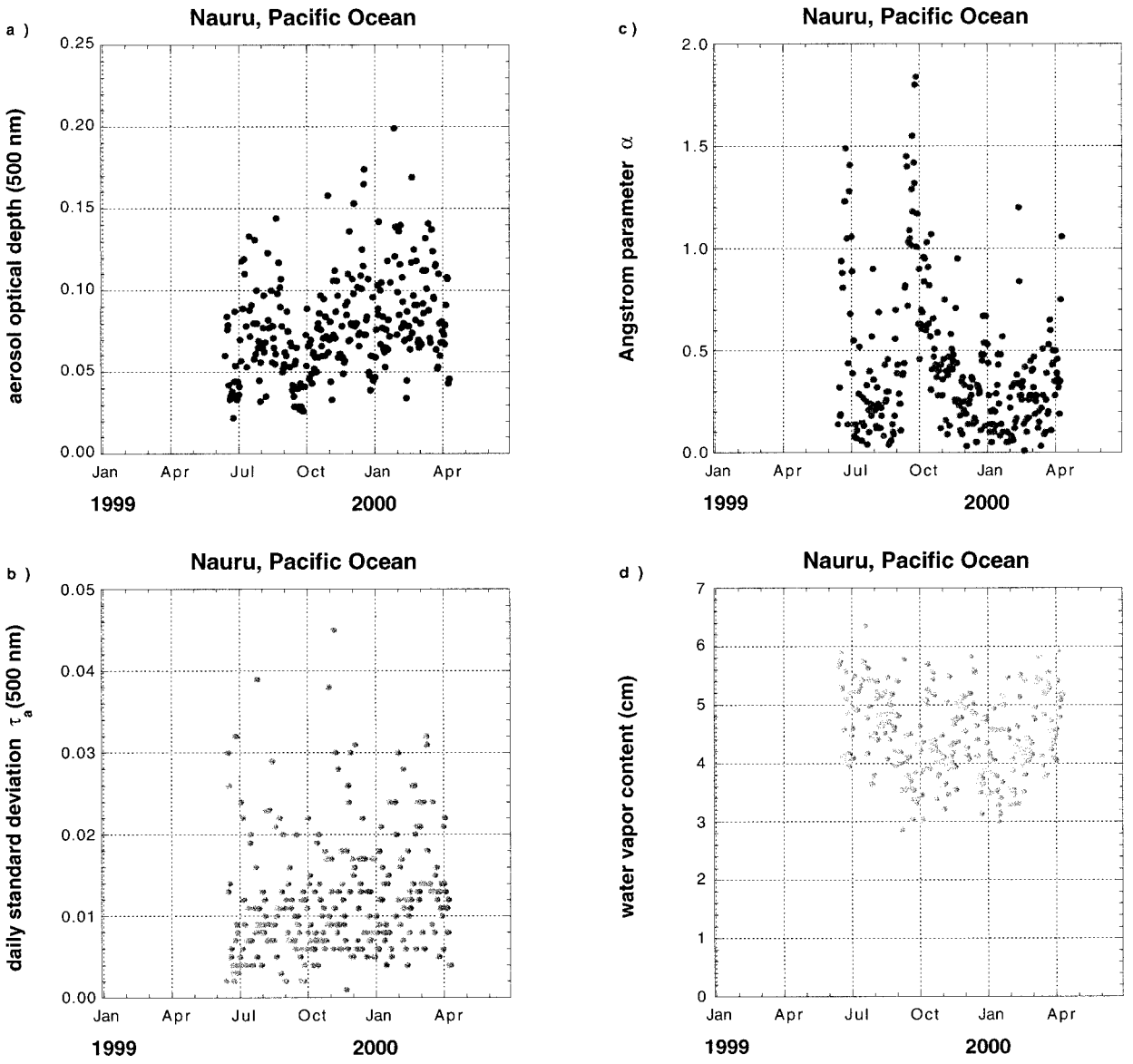

FIG. 2. Nauru (0°30′S, 166°54′E; elevation 7 m), Pacific Ocean. (a) Mean daily values of aerosol optical depth at 500 nm (b) daily std dev of τ_a(500 nm), (c) mean daily values of Ångstrõm parameter, and (d) WVC in the total atmospheric column.

The Ångström parameter is typically below 1 (Fig. 6c), which indicates that coarse particles (small αs) usually dominate the aerosol optical properties. Therefore, atmospheric optical conditions on Ascension are closer to background maritime conditions in comparison to Bermuda.

The frequency of occurrence distributions for τ_a and α are presented in Figs. 7 and 8. The frequency histograms of τ_a(500 nm) for the Pacific sites demonstrate that the majority of values (~75%–85%) are less than 0.10 (Figs. 7a–7c). The aerosol optical depth probability distributions for the Atlantic sites are relatively broader with the modal value of about 0.1. The most frequently occurring values of τ_a(500 nm) for all five sites are presented in Table 3.

The Ångström parameter frequency distribution for Nauru (Fig. 8) shows a relatively neutral spectral dependence of optical depth (modal value of $\alpha \sim 0.3$), for Lanai, Tahiti, and Ascension it has a peak around 0.7 with lesser frequencies trailing off at higher α values. The frequency histogram for Bermuda is slightly skewed towards higher α's with peak frequency at 0.9. The mode α values are listed in Table 3.

The scattergrams in Fig. 9 demonstrates how daily averages of aerosol optical depth correlate with the Ångström parameter α in the five sites. For Nauru data a wide range of α at low aerosol optical depths (<0.06) and the high negative correlation ($r = -0.75$) between them, reflects the increasing influence of a background fine aerosol on $\tau_a(\lambda)$ in a remote oceanic atmospheric

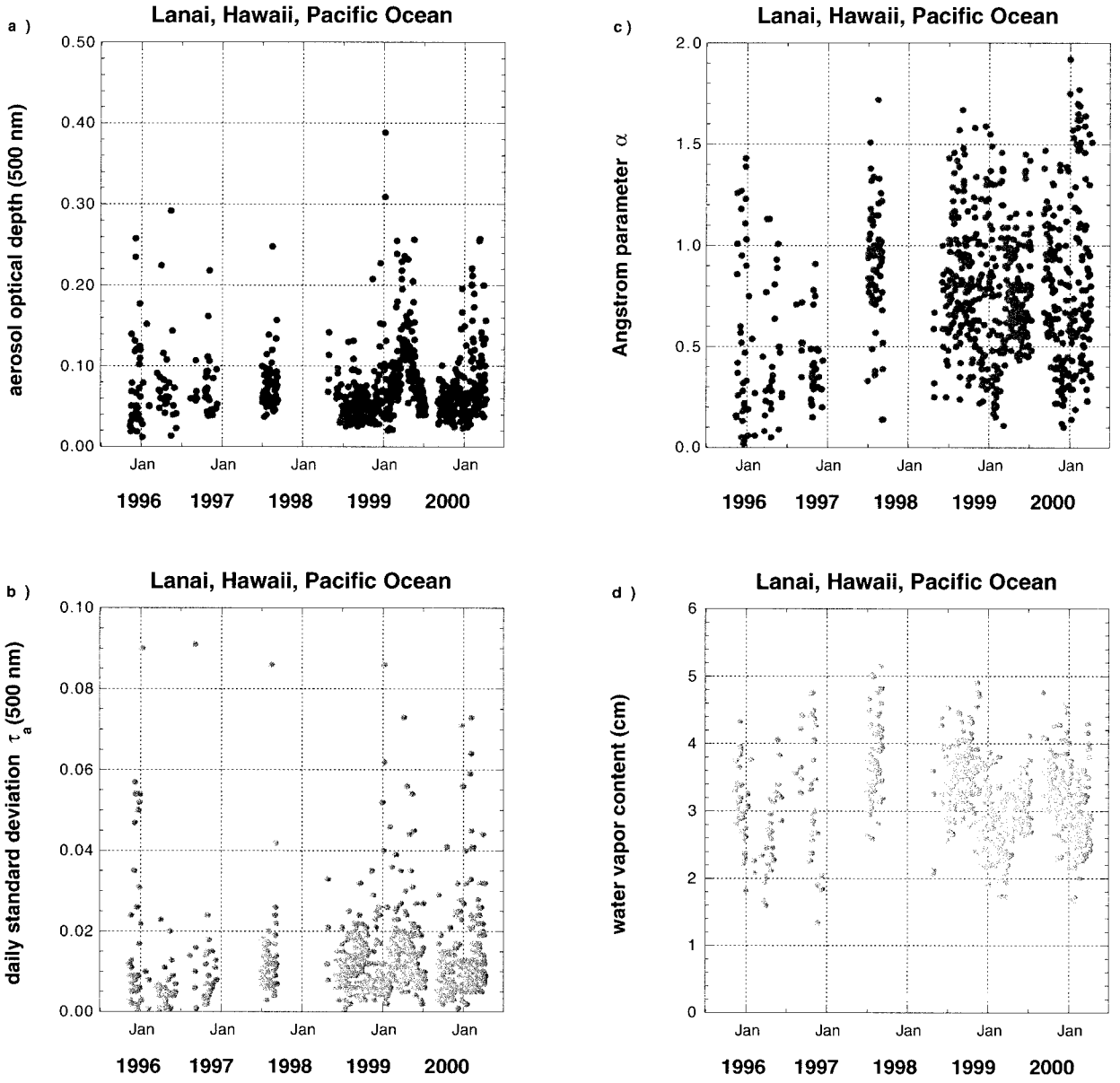

FIG. 3. Lanai, Hawaii (20°49′N, 156°59′W; elevation 20 m), Pacific Ocean. (a) Mean daily values of aerosol optical depth at 500 nm, (b) daily std dev of τ_a(500 nm), (c) mean daily values of Ångstrõm parameter, and (d) WVC in the total atmospheric column.

conditions. One can observe a weak trend of increasing values of α as τ_a(500 nm) decreases over Tahiti. Correlation between them, however, cannot be considered strong ($r = -0.39$, i.e., only 15% of variance explained), thus indicating simply a reasonable trend. A variety of optical conditions over Bermuda and Ascension can be seen in Fig. 9. Dusty conditions are separated from urban–industrial aerosol cluster by relatively clean maritime conditions.

b. Size distributions

Aerosol volume size distributions and single scattering albedos in the total atmospheric column were retrieved from sun and sky radiance measurements according to Dubovik and King (2000). In the retrieval algorithm the aerosol particles are assumed to be polydisperse homogeneous spheres. Robustness of the retrieved size distributions was assured by the residual error threshold [see formula (6) in Dubovik et al. 2000] of less than 5% (between computed and measured radiances) and by the number of scattering angles in the measured sky radiance distributions not less than 21 (Dubovik et al. 2002).

Figure 10 illustrates averaged size distributions ($dV/d\ln R$) for the five sites considered. Two modes are evident, a fine mode with radius $\sim<0.4$ μm and a coarse

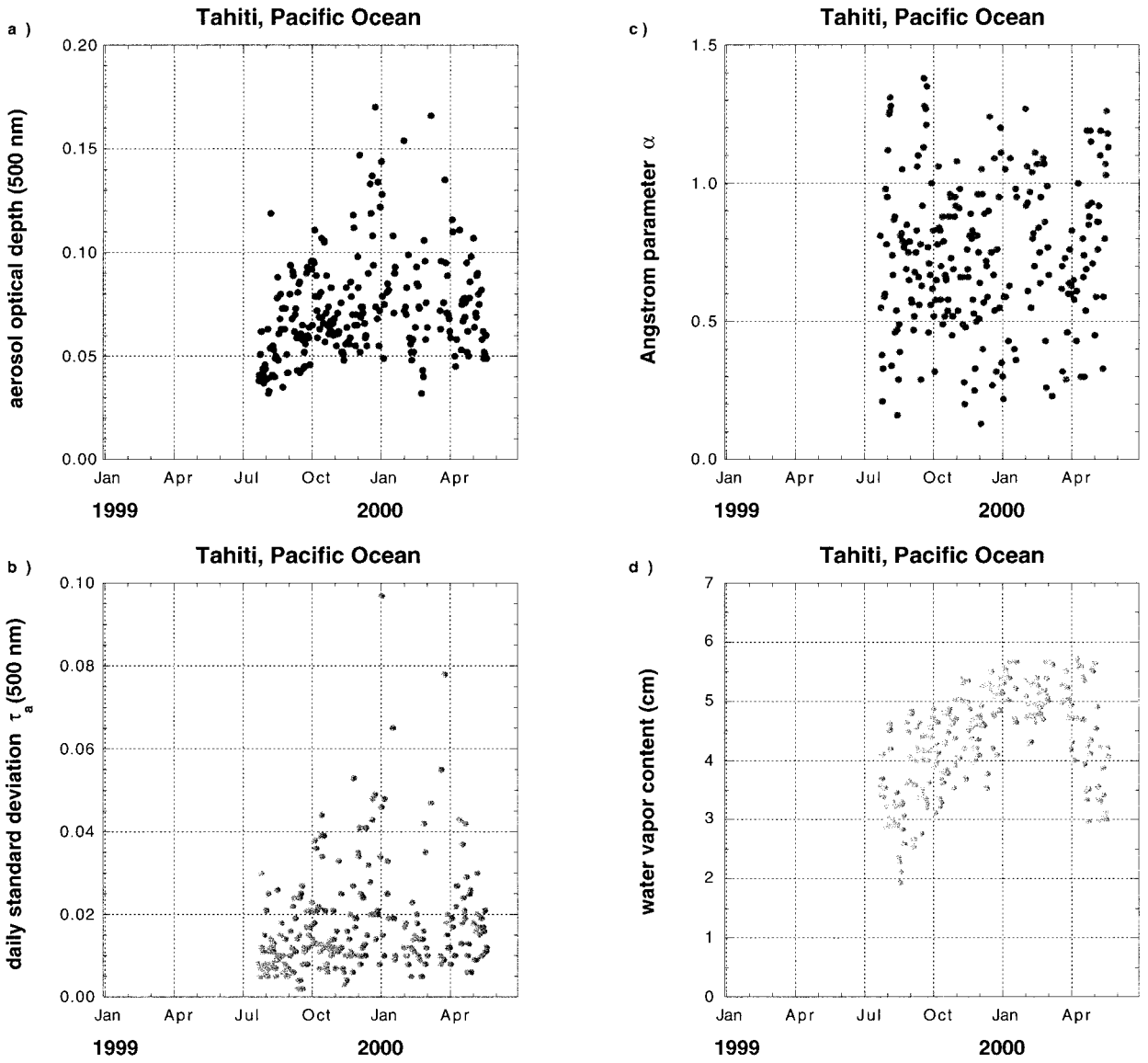

FIG. 4. As in Fig. 2 but for Tahiti (17°32′S, 149°34′W; elevation 98 m), Pacific Ocean, τ_a(500 nm).

mode with $r > 0.4$ μm. The dominant variations in these distributions can be directly associated with changes in the amplitude and spectral shape of the optical depth data [i.e., there is no significant influence of inversion artifacts due to nonspherisity (Dubovik et al. 2002)]. The volume size distributions in Fig. 10 clearly demonstrate the background natural aerosol optical properties over the Pacific sites and modified maritime aerosols over the Atlantic. The wide variety of optical conditions changed the shape of the coarse aerosol fraction on Bermuda.

Table 4 presents parameters of the bimodal lognormal volume size distributions (Whitby 1978) shown in Fig. 10. It should be noted that we assigned particles with radii $0.05 < r < 0.3 \div 0.6$ μm and with radii $0.3 \div 0.6 < r < 15$ μm to the fine and coarse modes respectively (before and after the infliction point). The effective radius is defined as a ratio of the third over the second moment of the size distribution. Volume concentrations for each fraction are also presented in Table 4.

Variations in aerosol volume size distributions over the Pacific were mainly due to changes in the concentration of the coarse aerosol fraction. Over the Atlantic the magnitude of the fine (accumulation) mode increased substantially, however, the relative contribution of the coarse mode is greater over Ascension than over Bermuda.

Parameters of the columnar aerosol size distributions listed in Table 4 are not inconsistent with the results obtained in situ (e.g., Hoppel et al. 1985; Hoppel and Frick 1990; Hoppel et al. 1990; and Table 2). Agreement of the fine-mode geometric mean radii is rather re-

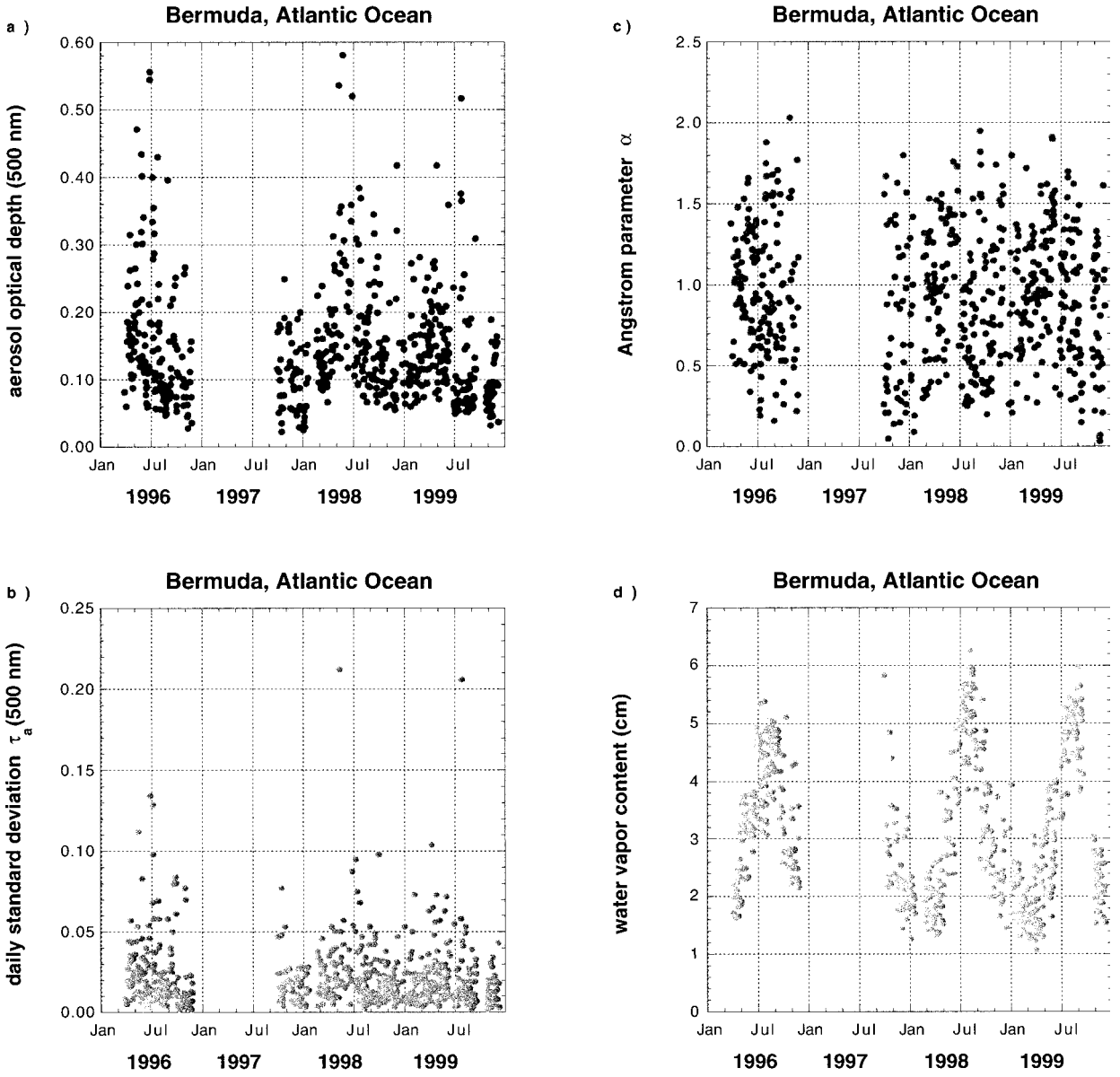

FIG. 5. As in Fig. 2 but for Bermuda (32°22′N, 64°41′W; elevation 10 m), Atlantic Ocean.

markable ($R_v \sim 0.1$–0.2 μm). Retrieved values for the coarse-mode radii are close to the models of Shettle and Fenn (1979), Porter and Clarke (1997), and the measurements of Horvath (1990), Kim et al. (1990), and Jennings et al. (1997). Measurement results reported by Quinn et al. (2001) for the Southern Atlantic temperate air are also consistent with our retrievals. Note that parameters presented in Table 4 describe aerosol size distributions in ambient conditions and are not associated with particular relative humidity levels.

We have to admit that one would not expect the ''dry'' mode parameters to agree with either the ambient in situ measurements in Table 2 or the derived ambient size distributions in Fig. 10. It was not possible to adjust parameters presented for the ''ambient'' conditions in Table 2 to the so-called dry conditions, simply because the ambient relative humidity was not known. In case of the columnar size distribution retrievals it simply cannot be done. Dry radius of about 0.10 μm would be expected to be 0.14 μm for the ''wet'' (relative humidity ~90%) aerosol. For lower relative humidity (70% and 80%) the ''humidity growth factor'' is 1.06 and 1.22, respectively (Shettle and Fenn 1979).

Single scattering albedo retrievals were inconclusive. SSA can hardly be retrieved in the conditions of low aerosol loading. Even the uncertainty of ± 0.01 in τ_a for small $\tau_a \leq 0.10$ becomes a significant obstacle for retrieving the imaginary part of the refractive index and

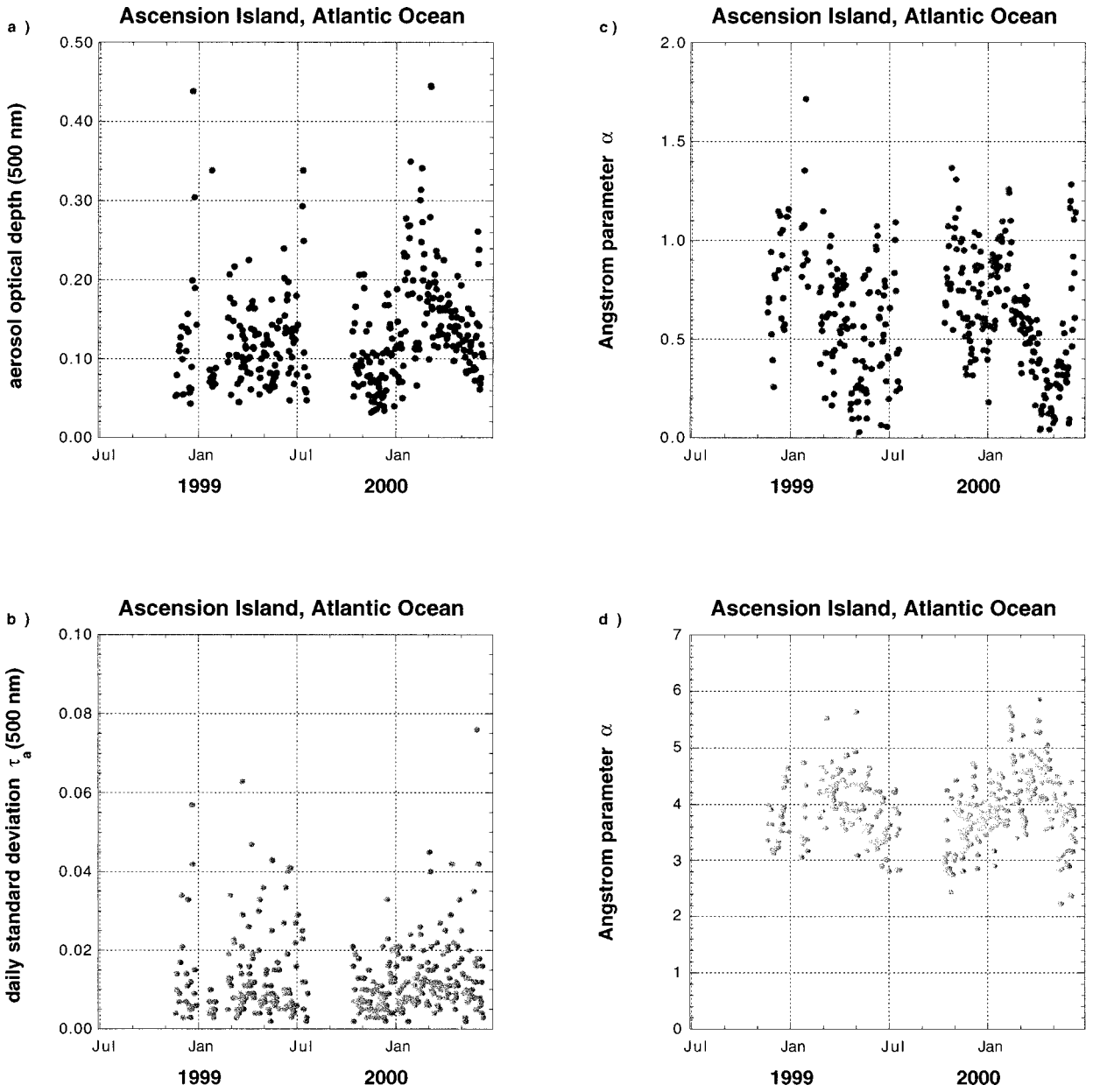

FIG. 6. As in Fig. 2, but for Ascension Island (7°56′S, 14°22′W; elevation 30 m), Atlantic Ocean.

SSA (Dubovik et al. 2000). More than 10% uncertainty in optical depth (in a sense of 0.01/0.10) is comparable with the absorption partition in total optical depth.

5. Summary

The principal conclusions drawn from our work can be summarized as follows.

1) A summary of aerosol optical depth measurements in a maritime environment during the last three decades was presented. The results of 75 publications were encapsulated in a single comprehensive table. Despite instrumental and calibration differences overall, aerosol optical depths over remote oceanic areas (not influenced by desert dust outbreaks or volcanic activity) according to Table 1, are, as a rule, smaller than 0.12. In coastal areas and inland seas values of aerosol optical depth are higher, largely depending on continental sources. It is, however, noted that high-latitude oceanic data are underrepresented.
2) A short summary of the more recent in situ measurements of aerosol size distributions over the oceans was presented (Table 2). Parameters of aero-

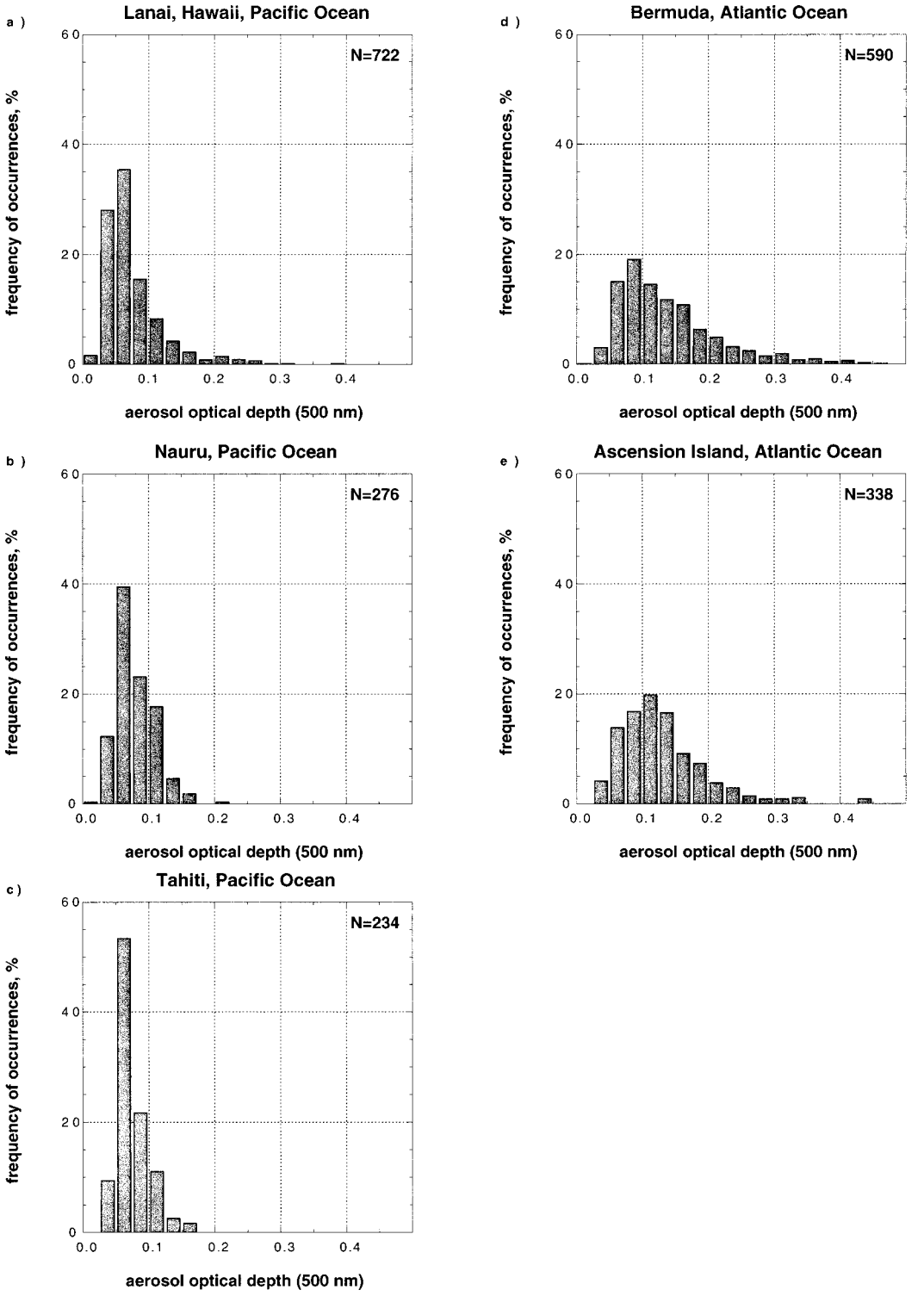

FIG. 7. Frequency of occurrences of aerosol optical depth at 500 nm for (a) Lanai, (b) Nauru, (c) Tahiti, (d) Bermuda, and (e) Ascension Island.

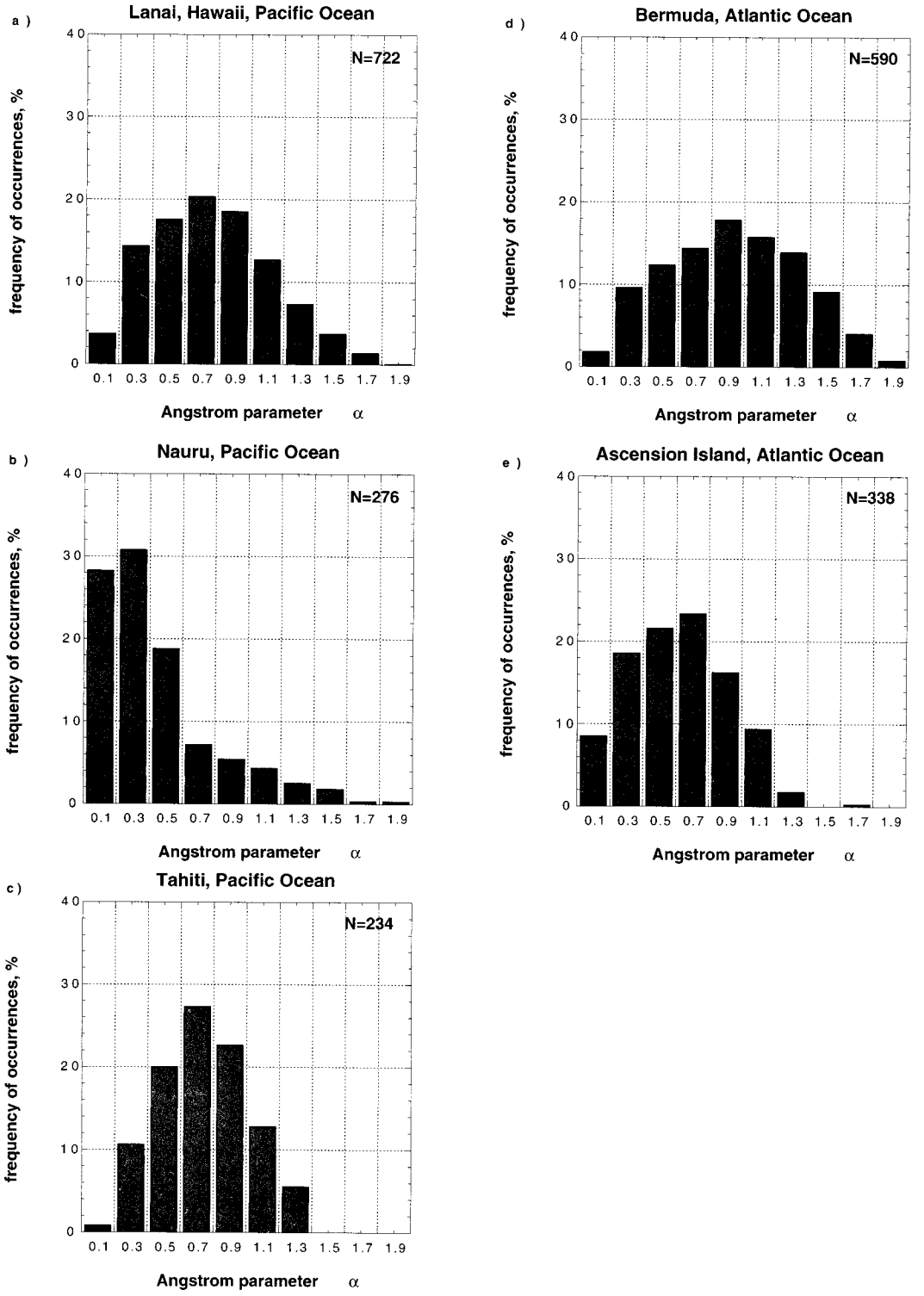

FIG. 8. Frequency of occurrences of Ångström parameter for (a) Lanai, (b) Nauru, (c) Tahiti, (d) Bermuda, and (e) Ascension Island.

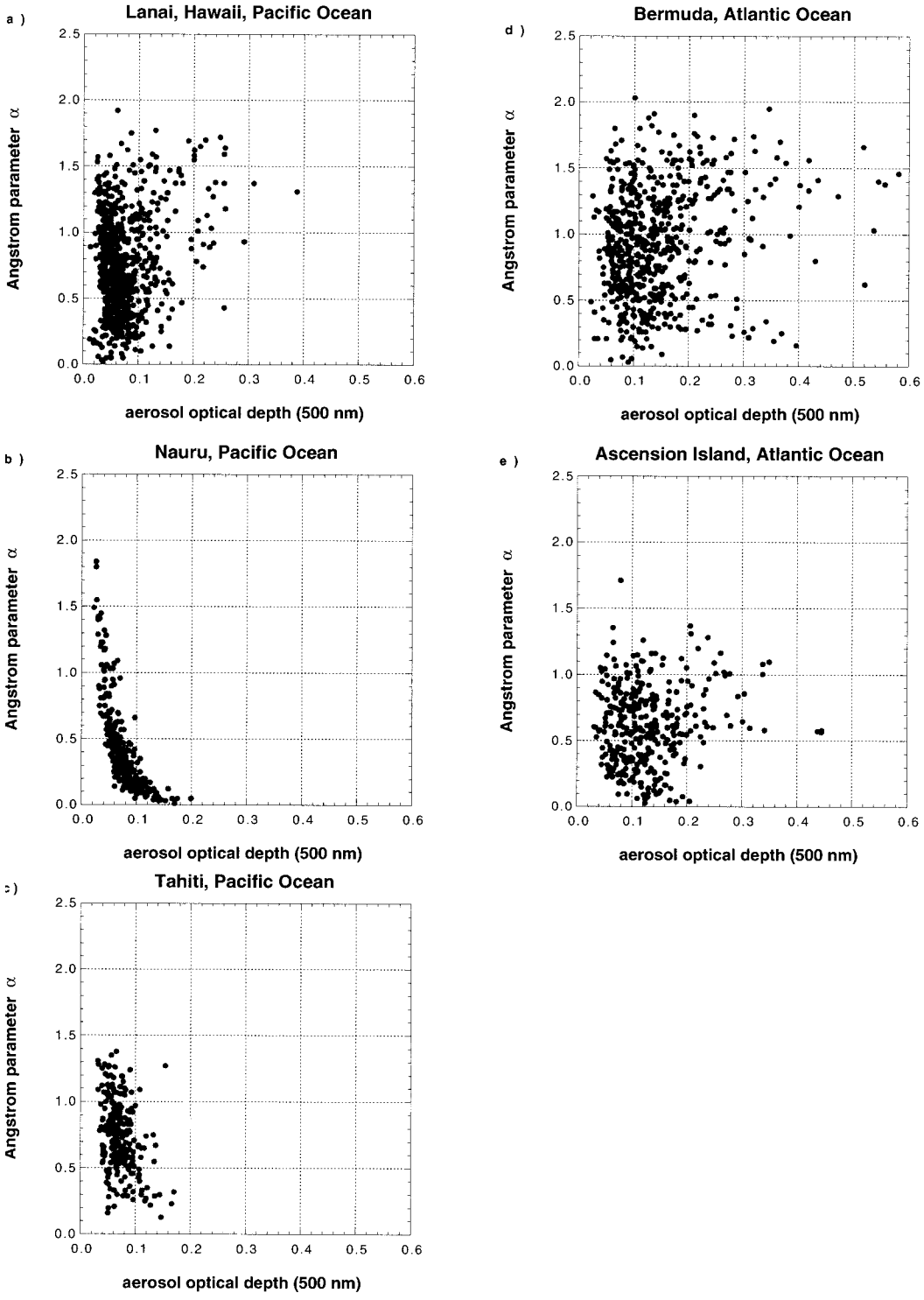

FIG. 9. Scattergrams of Ångström parameter versus aerosol optical depth for (a) Lanai, (b) Nauru, (c) Tahiti, (d) Bermuda, and (e) Ascension Island.

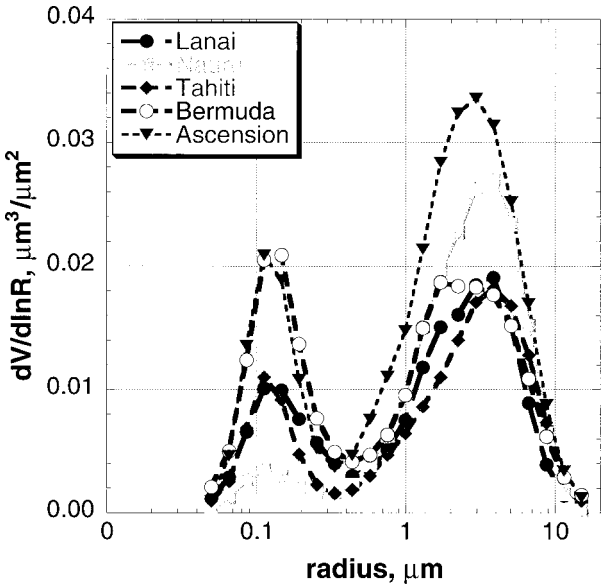

FIG. 10. Average aerosol volume size distributions in the total atmospheric column.

sol volume size distributions showed good agreement for the fine-mode aerosol, however the coarse-mode parameters indicated substantial differences.

3) Daily statistics for aerosol optical depth, Ångström parameter and precipitable water have been computed for five AERONET island sites. Background levels of aerosols, which we define as τ_a(500 nm) less than 0.10 were dominant at all five sites but with varying frequencies. Aerosol over the Pacific Ocean (three sites at 20°S to 20°N) still resembles mostly clean maritime aerosol mainly free of continental influences. The optical depth is stable with mean value of τ_a(500 nm) = 0.07, mode value at τ_{am} = 0.06, and standard deviation of 0.02 to 0.05. The Ångström parameter ranging 0.3 to 0.7 characterizes the wavelength dependence of the optical depth. Over the Atlantic (two stations at 7°S and 32°N) the optical thickness is significantly higher: τ_a(500 nm) = 0.14 and τ_{am} = 0.10, due to the frequent presence of dust, smoke, and urban–industrial aerosol. It is notable, that the mean τ_a(500 nm) value of 0.07 over the Pacific Ocean agrees with recently calculated optical thickness of 0.07 for the natural component of aerosol in the polluted Indian Ocean, based on chemical analysis (Ramanathan et al. 2001).
4) The volume size distributions clearly demonstrate the background natural aerosol optical properties over the Pacific Ocean sites and modified maritime aerosols over the Atlantic. Variations in the size distributions over the Pacific were mainly due to changes in the concentration of the coarse aerosol fraction, however, over the Atlantic the magnitude of the fine (accumulation) mode increased substantially. The atmospheric column aerosol is characterized by a bimodal lognormal size distribution with a fine mode at $R_{\text{eff}} = 0.11 \pm 0.01$ μm and coarse mode at $R_{\text{eff}} = 2.3 \pm 0.2$ μm over the Pacific and $R_{\text{eff}} = 1.9 \pm 0.1$ μm over the Atlantic.

Acknowledgments. The authors thank Dr. Robert Curran of NASA headquarters (Radiation Sciences Program) and Dr. Michael King of the EOS Project Science Office for their support of AERONET. We also thank the NASA SIMBIOS project (Dr. C. McClain and Dr. G. Fargion) for its financial support in establishing and maintaining sites on Tahiti, Lanai, and Ascension Island. Brookhaven National Laboratory is acknowledged for its support of the site in Nauru. We thank Dr. Dennis Clark, NOAA, for his effort in establishing and maintaining Lanai site. Thanks are also extended to the staff of Bermuda Biological Station for maintaining the site. We acknowledge the critical effort of AERONET team member Wayne Newcomb. The authors would also like to acknowledge the constructive criticism of anonymous reviewers.

REFERENCES

Adnashkin, V. N., L. K. Veselova, O. D. Barteneva, N. I. Nikitinskaya, and A. G. Laktionov, 1979: Atmospheric optical characteristics in the tropical zone of the Atlantic ocean (English translation). *Sov. Meteor. Hydrol.,* **N11,** 49–54.

TABLE 4. Parameters of aerosol volume size distributions.

	Fine mode				Coarse mode				
	C_V[a]	R_V[b]	R_{eff}[c]	σ[d]	C_V[b]	R_V[b]	R_{eff}[c]	σ[d]	N[e]
Lanai	0.014	0.15	0.12	0.57	0.035	2.74	2.09	0.74	784
Nauru	0.004	0.13	0.11	0.49	0.049	2.93	2.26	0.72	36
Tahiti	0.010	0.12	0.11	0.38	0.034	3.29	2.44	0.78	148
Bermuda	0.024	0.14	0.12	0.46	0.041	2.55	1.80	0.83	200
Ascension	0.021	0.13	0.12	0.40	0.066	2.62	1.93	0.78	66

[a] C_V is the columnar volume of particles per unit cross section of atmospheric column ($\mu m^3/\mu m^2$).
[b] R_V is the volume geometric mean radius (μm).
[c] R_{eff} is the effective radius (μm).
[d] σ is the geometric standard deviation.
[e] N is the number of averaged retrievals.

Afonin, Y. I., 1983: Investigation on optical characteristics of maritime atmosphere (in Russian). *Abstracts, Third All-Union Conf. on Atmospheric Optics and Actinometry,* Part 1, Tomsk, Russia, Institute of Atmospheric Optics, 58–60.

Artemkin, E. E., and S. I. Krivoshein, 1983a: Statistical characteristics of atmospheric optical parameters over the water areas influenced by continent (in Russian). *Abstracts, Third All-Union Conf. on Atmospheric Optics and Actinometry,* Part 1, Tomsk, Russia, Institute of Atmospheric Optics, 277–279.

——, and ——, 1983b: Statistical models of variability of the spectral structure of aerosol optical depths and polarization degrees of light scattered by the atmosphere over the background regions of the Atlantic ocean (in Russian). *Abstracts, Third All-Union Conf. on Atmospheric Optics and Actinometry,* Part 1, Tomsk, Russia, Institute of Atmospheric Optics, 274–276.

——, ——, and S. G. Moiseev, 1980: Statistical characteristics of the spectral structure of aerosol optical depths (in Russian). *Abstracts, Second All-Union Conf. on Atmospheric Optics,* Part 1, Tomsk, Russia, Institute of Atmospheric Optics, 134–136.

Barteneva, O. D., L. K. Veselova, and N. I. Nikitinskaya, 1974: On the optical properties of atmospheric aerosols in the tropical zone of the Atlantic Ocean (in Russian). *Tropeks-72,* Gidrometeoizdat, 482–494.

——, N. I. Nikitinskaya, G. G. Sakunov, and L. K. Veselova, 1991: *Atmospheric Transmittance in the Visible and Near IR Spectral Range* (in Russian). Gidrometeoizdat, 224 pp.

Bates, T. S., B. J. Huebert, J. L. Gras, F. B. Griffiths, and P. A. Durkee, 1998a: International Global Atmospheric Chemistry (IGAC) Project's First Aerosol Characterization Experiment (ACE 1): Overview. *J. Geophys. Res.,* **103,** 16 297–16 318.

——, and Coauthors, 1998b: Processes controling the distribution of aerosol particles in the lower marine boundary layer during the First Aerosol Characterization Experiment (ACE 1). *J. Geophys. Res.,* **103,** 16 369–16 383.

——, P. K. Quinn, D. S. Covert, D. J. Coffman, J. E. Johnson, and A. Wiedensohler, 2000: Aerosol physical properties and processes in the lower marine boundary layer: A comparison of shipboard sub-micron data from ACE-1 and ACE-2. *Tellus,* **52B,** 258–272.

Blanchard, D. C., and A. H. Woodcock, 1980: The production, concentration, and vertical distribution of the sea-slat aerosol. *Ann. N. Y. Acad. Sci.,* **338,** 330–347.

Bodhaine, B. A., B. G. Mendonca, J. M. Harris, and J. M. Miller, 1981: Seasonal variations in aerosols and atmospheric transmission at Mauna Loa Observatory. *J. Geophys. Res.,* **86,** 7395–7398.

Brechtel, F. J., S. M. Kreidenweis, and H. B. Swan, 1998: Air mass characteristics, aerosol particle number concentrations, and number size distributions at Macquarie Island during the First Aerosol Characterization Experiment (ACE 1). *J. Geophys. Res.,* **103,** 16 351–16 367.

Burmistrova, V. D., and G. L. Shubova, 1974: Aerosol atmospheric transmittance in tropical zones of the Atlantic and Pacific oceans (in Russian). *Hydrophysical and Hydrooptical Studies in the Atlantic and Pacific Oceans,* Nauka, 293–297.

Charlson, R. J., S. E. Schwartz, J. M. Hales, R. D. Cess, J. A. Coakley Jr., J. E. Hansen, and D. J. Hofmann, 1992: Climate forcing by anthropogenic aerosols. *Science,* **255,** 423–430.

Clarke, A. D., and J. N. Porter, 1994: Aerosol measurements and optical extinction in the marine boundary layer. *Proc., Int. Specialty Conf. on Aerosols and Atmospheric Optics: Radiative Balance and Visual Air Quality,* Vol. 4, Snowbird, UT, Air and Waste Management Association, 209–226.

de Leeuw, G., 1991: Aerosol models for optical and IR propagation in the marine atmospheric boundary layer. *Proc. SPIE,* **1487,** 130–159.

Deuze, J. L., C. Devaux, M. Herman, R. Santer, and D. Tanre, 1988: Saharan aerosols over the south of France: Characterization derived from satellite data and ground based measurements. *J. Appl. Meteor.,* **27,** 680–686.

Dubovik, O., and M. D. King, 2000: A flexible inversion algorithm for retrieval of aerosol optical properties from sun and sky radiance measurements. *J. Geophys. Res.,* **105,** 20 673–20 696.

——, A. Smirnov, B. N. Holben, M. D. King, Y. J. Kaufman, T. F. Eck, and I. Slutsker, 2000: Accuracy assessments of aerosol optical properties retrieved from AERONET sun and sky radiance measurements. *J. Geophys. Res.,* **105,** 9791–9806.

——, B. N. Holben, T. F. Eck, A. Smirnov, Y. J. Kaufman, M. D. King, D. Tanré, and I. Slutsker, 2002: Variability of absorption and optical properties of key aerosol types observed in worldwide locations. *J. Atmos. Sci.,* **59,** 590–608.

Eck, T. F., B. N. Holben, J. S. Reid, O. Dubovik, A. Smirnov, N. T. O'Neill, I. Slutsker and S. Kinne, 1999: Wavelength dependence of the optical depth of biomass burning, urban, and desert dust aerosol. *J. Geophys. Res.,* **104,** 31 333–31 350.

——, ——, O. Dubovik, A. Smirnov, I. Slutsker, J. M. Lobert, and V. Ramanathan, 2001: Column integrated aerosol optical properties over the Maldives during the NE monsoon for 1998–2000. *J. Geophys. Res.,* **106,** 28 555–28 566.

Eerme, K. A., 1983: Atmospheric and optical studies in the Baltic Sea from a board of research vessel *Ayu-Dag* in the summer of 1981 (in Russian). *Studies of Variability of Optical Properties of the Baltic Sea,* Tallinn, 43–57.

Emelyanov, V. N., S. L. Kislitsin, and S. A. Ilyicheva, 1978: Observations of spectral aerosol optical depths of atmosphere in the 28th cruise of research vessel *Professor Vize* (in Russian). *Aerosol Optics,* Ryazan, 23–28.

Fischer, W. H., 1967: Some atmospheric turbidity measurements in Antarctica. *J. Appl. Meteor.,* **6,** 938–939.

Fitzgerald, J. M., 1991: Marine aerosols: A review. *Atmos. Environ.,* **25A,** 533–545.

Fraser, R. S., 1976: Satellite measurements of mass of Sahara dust in the atmosphere. *Appl. Opt.,* **15,** 2471–2479.

Gashko, V. A., and K. S. Shifrin, 1983: Spectral transmittance of atmosphere in northwestern part of the Pacific Ocean (in Russian). *Marine Optics,* K. S. Shifrin, Ed., Nauka, 190–194.

Gathman, S. G., 1983: Optical properties of the marine aerosol as predicted by the Navy aerosol model. *Opt. Eng.,* **22,** 57–62.

Gras, J. L., 1995: CN, CNN and particle size in Southern Ocean air at Cape Grim. *Atmos. Res.,* **35,** 233–251.

Guschin, G. K., 1970: Optical characteristics of aerosols over the oceans (in Russian). *Tr. Gl. Geofiz. Obs.,* **255,** 52–68.

Guttman, A., 1968: Extinction coefficient measurements of clear atmospheres and cirrus clouds. *Appl. Opt.,* **7,** 2377–2381.

Haggerty, J. A., P. A. Durkee, and B. J. Wattle, 1990: A comparison of surface and satellite-derived aerosol measurements in the western Mediterranean. *J. Geophys. Res.,* **95,** 1547–1557.

Hansen, J., M. Sato, and R. Ruedy, 1997: Radiative forcing and climate response. *J. Geophys. Res.,* **102,** 6831–6864.

——, ——, ——, A. Lacis, and V. Oinas, 2000: Global warming in the twenty-first century: An alternative scenario. *Proc. Natl. Acad. Sci. U.S.A.,* **97,** 9875–9880.

Hayasaka, T., N. Iwasaka, G. Hashida, I. Takizawa, and M. Tanaka, 1994: Changes in stratospheric aerosols and solar insolation due to Mt. Pinatubo eruption as observed over the western Pacific. *Geophys. Res. Lett.,* **21,** 1137–1140.

Herman, J., P. K. Bhartia, O. Torres, N. C. Hsu, C. J. Seftor, and E. Celarier, 1997: Global distribution of UV-absorbing aerosols from Nimbus 7/TOMS data. *J. Geophys. Res.,* **102,** 16 911–16 921.

Hess, M., P. Koepke, and I. Schult, 1998: Optical properties of aerosols and clouds: The software package OPAC. *Bull. Amer. Meteor. Soc.,* **79,** 831–844.

Hogan, A. W., 1981: Aerosol measurements over and near the south Pacific Ocean and Ross Sea. *J. Appl. Meteor.,* **20,** 1111–1118.

Holben, B. N., and Coauthors, 1998: AERONET—A federated instrument network and data archive for aerosol characterization. *Remote. Sens. Environ.,* **66,** 1–16.

——, and Coauthors, 2001: An emerging ground based aerosol climatology: Aerosol optical depth from AERONET. *J. Geophys. Res.,* **106,** 12 067–12 097.

Hoppel, W. A., and G. M. Frick, 1990: Submicron aerosol size dis-

tributions measured over the tropical and South Pacific. *Atmos. Environ.*, **24A,** 645–659.
——, J. W. Fitzgerald, and R. E. Larson, 1985: Aerosol size distributions in air masses advecting off the East Coast of the United States. *J. Geophys. Res.*, **90,** 2365–2379.
——, ——, G. M. Frick, R. E. Larson, and E. J. Mack, 1990: Aerosol size distributions and optical properties found in the marine boundary layer over the Atlantic Ocean. *J. Geophys. Res.*, **95,** 3659–3686.
Horvath, H., R. L. Gunter, and S. W. Wilkinson, 1990: Determination of the coarse mode of the atmospheric aerosol using data from a forward-scattering spectrometer probe. *Aerosol Sci. Technol.*, **12,** 964–980.
Husar, R. B., J. M. Prospero, and L. L. Stowe, 1997: Characterization of tropospheric aerosols over the oceans with the NOAA advanced very high resolution radiometer optical thickness operational product. *J. Geophys. Res.*, **102,** 16 889–16 909.
Ignatov, A. M., I. L. Dergileva, S. M. Sakerin, and D. M. Kabanov, 1993: An algorithm for the sun photometer calibration. *Proc. IGARSS' 93 Symp.*, Tokyo, Japan, IEEE, 1091–1093.
IPCC, 1994: *Radiative Forcing of Climate*. Cambridge University Press.
Jaenicke, R., and L. Schutz, 1978: Comprehensive study of physical and chemical properties of the surface aerosol in the Cape Verde islands region. *J. Geophys. Res.*, **83,** 3585–3599.
Jankowiak, I., and D. Tanre, 1992: Satellite climatology of Saharan dust outbreaks: Method and preliminary results. *J. Climate*, **5,** 646–656.
Jennings, S. G., and C. D. O'Dowd, 1990: Volatility of aerosol at Mace Head, on the west coast of Ireland. *J. Geophys. Res.*, **95,** 13 937–13 948.
——, M. Geever, F. M. McGovern, J. Francis, T. G. Spain, and T. Donaghy, 1997: Microphysical and physico-chemical characterization of atmospheric marine and continental aerosol at Mace Head. *Atmos. Environ.*, **31,** 2795–2808.
Junge, C. E., 1972: Our knowledge of the physico-chemistry of aerosols in the undisturbed marine environment. *J. Geophys. Res.*, **77,** 5183–5200.
Karimova, G. U., 1976: Measurement results for ozone and optical characteristics of atmosphere over the North Atlantic (in Russian). *Tr. Arct. Antarct. Inst.*, **327,** 209–214.
Kaufman, Y. J., 1993: Aerosol optical thickness and atmospheric path radiance. *J. Geophys. Res.*, **98,** 2677–2692.
——, and Coauthors, 1998: Smoke, clouds, and radiation—Brazil (SCAR-B) experiment. *J. Geophys. Res.*, **103,** 31 783–31 808.
——, A. Smirnov, B. N. Holben, and O. Dubovik, 2001: Baseline maritime aerosol: Methodology to derive the optical thickness and scattering properties. *Geophys. Res. Lett.*, **28,** 3251–3254.
Kiehl, J. T., and B. P. Briegleb, 1993: The relative roles of sulfate aerosols and greenhouse gases in climate forcing. *Science*, **260,** 311–314.
Kim, Y., H. Sievering, and J. Boatman, 1990: Volume and surface area size distribution, water mass and model fitting of GCE/CASE/WATOX marine aerosols. *Global Biochem. Cycles*, **4,** 165–177.
——, ——, ——, D. Wellman, and A. Pszenny, 1995: Aerosol size distribution and aerosol water content measurements during Atlantic Stratocumulus Transition Experiment/Marine Aerosol and Gas Exchange. *J. Geophys. Res.*, **100,** 23 027–23 038.
King, M. D., and D. M. Byrne, 1976: A method for inferring total ozone content from spectral variation of total optical depth obtained with a solar radiometer. *J. Atmos. Sci.*, **33,** 2242–2251.
——, Y. J. Kaufman, D. Tanre, and T. Nakajima, 1999: Remote sensing of tropospheric aerosols from space: Past present and future. *Bull. Amer. Meteor. Soc.*, **80,** 2229–2259.
Knestrick, G. L., and Coauthors, 1962: Atmospheric scattering coefficients in the visible and infrared regions. *J. Opt. Soc. Amer.*, **52,** 1010–1016.
Korotaev, G. K., S. M. Sakerin, A. M. Ignatov, L. L. Stowe, and E. P. McClain, 1993: Sun-photometer observations of aerosol optical thickness over the North Atlantic from a Soviet research vessel for validation of satellite measurements. *J. Atmos. Oceanic Technol.*, **10,** 725–735.
Kusmierczyk-Michulec, J., and M. Darecki, 1996: The aerosol optical thickness over the Baltic Sea. *Oceanologia*, **38,** 423–435.
——, O. Kruger, and R. Marks, 1999: Aerosol influence on the sea-viewing wide-field-of-view sensor bands: Extinction measurements in a marine summer atmosphere over the Baltic Sea. *J. Geophys. Res.*, **104,** 14 293–14 307.
Kuznetsov, G. I., and N. I. Izhovkina, 1973: Two models of atmospheric aerosol (English translation). *Izv. Acad. Sci. USSR Atmos. Oceanic Phys.*, **9,** 537–540.
Livingston, J. M., and Coauthors, 2000: Shipboard sunphotometer measurements of aerosol optical depth spectra and columnar water vapor during ACE-2 and comparison with selected land, ship, aircraft, and satellite measurements. *Tellus*, **52B,** 593–618.
Lukyanchikova, N. A., and A. A. Govorushkin, 1981: Spectral characteristics of atmosphere over the northern part of the Atlantic Ocean (in Russian). *Tr. Arct. Antarct. Inst.*, **370,** 160–164.
Masuda, K., M. Sasaki, T. Takashima, and H. Ishida, 1999: Use of polarimetric measurements of the sky over the ocean for spectral optical thickness retrievals. *J. Atmos. Oceanic Technol.*, **16,** 846–859.
Mather, J. H., T. P. Ackerman, W. E. Clements, F. J. Barnes, M. D. Ivey, L. D. Hatfield, and R. M. Reynolds, 1998: An atmospheric radiation and cloud station in the tropical western Pacific. *Bull. Amer. Meteor. Soc.*, **79,** 627–642.
Matsubara, K., T. Ohata, and S. Kawaguchi, 1983: Turbidity over the Indian Ocean. *Proceedings of the Fifth Symposium on Polar Meteorology and Glaciology*, Special Issue 29, Memoirs of the National Institute of Polar Research, 77–84.
McClain, C. R., and G. Fargion, 1999: SIMBIOS Project 1999 annual report. NASA Goddard Space Flight Center Tech. Memo. 1999-209486, 128 pp.
Mishchenko, M. I., I. V. Geogdzhayev, B. Cairns, W. B. Rossow, and A. A. Lacis, 1999: Aerosol retrievals over the ocean by use of channels 1 and 2 AVHRR data: Sensitivity analysis and preliminary results. *Appl. Opt.*, **38,** 7325–7341.
Moorthy, K. K., and A. Saha, 2000: Aerosol study during INDOEX: Observation of enhanced aerosol activity over the mid Arabian Sea during the northern winter. *J. Atmos. Sol. Terr. Phys.*, **62,** 65–72.
——, and S. K. Satheesh, 2000: Characteristics of aerosols over a remote island, Minicoy in the Arabian Sea: Optical properties and retrieved size characteristics. *Quart. J. Roy. Meteor. Soc.*, **126,** 81–109.
——, P. R. Nair, and B. V. Krishna Murthy, 1991: Size distribution of coastal aerosols: Effects of local sources and sinks. *J. Appl. Meteor.*, **30,** 844–852.
——, S. K. Satheesh, and B. V. Krishna Murthy, 1997: Investigations of marine aerosols over the tropical Indian Ocean. *J. Geophys. Res.*, **102,** 18 827–18 842.
Moulin, C., F. Dulac, C. E. Lambert, P. Chazette, I. Jankowiak, B. Chatenet, and F. Lavenu, 1997: Long-term daily monitoring of Saharan dust load over ocean using Meteosat ISCCP-B2 data. 2. Accuracy of the method and validation using Sun photometer measurements. *J. Geophys. Res.*, **102,** 16 959–16 969.
Murayama, T., H. Okamoto, N. Kaneyasu, H. Katamaki, and K. Miura, 1999: Application of lidar depolarization measurement in the atmospheric boundary layer: Effects of dust and sea-salt particles. *J. Geophys. Res.*, **104,** 31 781–31 792.
O'Dowd, C. D., M. H. Smith, and S. R. Jennings, 1993: Submicron particles, radon, and soot carbon characteristics over the north-east Atlantic. *J. Geophys. Res.*, **98,** 1123–1135.
——, ——, I. E., Consterdine, and J. A. Lowe, 1997: Marine aerosol, sea-salt, and the marine sulphur cycle: A short review. *Atmos. Environ.*, **31,** 73–80.
O'Neill, N. T., T. F. Eck, B. N. Holben, A. Smirnov, O. Dubovik, and A. Royer, 2001: Uni and bi-modal size distribution influences on the variation of Angstrom derivatives in spectral and optical depth space. *J. Geophys. Res.*, **106,** 9787–9806.
Patterson, E. M., C. S. Kiang, A. C. Delany, A. F. Wartburg, A. C.

D. Leslie, and B. J. Huebert, 1980: Global measurements of aerosols in remote continental and marine regions: Concentrations, size distributions, and optical properties. *J. Geophys. Res.*, **85,** 7361–7376.

Penner, J. E., and Coauthors, 1994: Quantifying and minimizing uncertainty of climate forcing by anthropogenic aerosols. *Bull. Amer. Meteor. Soc.*, **75,** 375–400.

Perry, K. D., T. A. Cahill, R. C. Schnell, and J. M. Harris, 1999: Long-range transport of anthropogenic aerosols to the National Oceanic and Atmospheric Administration baseline station at Mauna Loa Observatory, Hawaii. *J. Geophys. Res.*, **104,** 18 521–18 533.

Platt, C. M. R., and G. R. Patterson, 1986: The interpretation of baseline atmospheric turbidity measurements at Cape Grim, Tasmania. *J. Atmos. Chem.*, **4,** 187–197.

Podzimek, J., 1980: Advances in marine aerosol research. *J. Rech. Atmos.*, **14,** 35–61.

Porter, J. N., and A. D. Clarke, 1997: Aerosol size distribution models based on in situ measurements. *J. Geophys. Res.*, **102,** 6035–6045.

——, M. Miller, C. Pietras, and C. Motell, 2001: Ship-based photometer measurements using Microtops sun photometers. *J. Atmos. Oceanic Technol.*, **18,** 765–774.

Price, S., 1983: *Atlas of Hawaii.* University of Hawaii Press.

Pueschel, R. F., J. M. Livingston, G. V. Ferry, and T. E. DeFelice, 1994: Aerosol abundances and optical characteristics in the Pacific basin free troposphere. *Atmos. Environ.*, **28,** 951–960.

Quenzel, H., 1970: Determination of size distribution of atmospheric aerosol particles from spectral solar radiation measurements. *J. Geophys. Res.*, **75,** 2915–2921.

Quinn, P. K., S. F. Marshall, T. S. Bates, D. S. Covert, and V. N. Kapustin, 1995: Comparison of measured and calculated aerosol properties relevant to the direct radiative forcing of tropospheric sulfate aerosol on climate. *J. Geophys. Res.*, **100,** 8977–8991.

——, V. N. Kapustin, T. S. Bates, and D. S. Covert, 1996: Chemical and optical properties of marine boundary layer aerosol particles of the mid-Pacific in relation to sources and meteorological transport. *J. Geophys. Res.*, **101,** 6931–6951.

——, D. J. Coffman, T. S. Bates, T. L. Miller, J. E. Johnson, K. Voss, E. J. Welton, and C. Neususs, 2001: Dominant aerosol chemical components and their contribution to extinction during the AEROSL99 cruise across the Atlantic. *J. Geophys. Res.* **106,** 20 783–20 810.

Raes, F., T. Bates, F. McGovern, and M. Van Liedekerke, 2000: The 2nd Aerosol Characterization Experiment (ACE-2): General overview and main results. *Tellus*, **52B,** 111–125.

Ramanathan, V., and Coauthors, 1995: Indian Ocean Experiment (INDOEX) White Paper. INDOEX Publ. 2, Scripps Institution of Oceanography.

——, and Coauthors, 2001: The Indian Ocean Experiment: An integrated assessment of the climate forcing and effects of the great Indo-Asian haze. *J. Geophys. Res.*, **106,** 28 371–28 398.

Reddy, P. L., F. W. Kreiner, J. J. DeLuisi, and Y. Kim, 1990: Aerosol optical depths over the Atlantic derived from shipboard sunphotometer observations during the 1988 global change expedition. *Global Biogeochem. Cycles*, **4,** 225–240.

Reid, J. S., H. H. Jonsson, M. H. Smith, and A. Smirnov, 2001: Evolution of the vertical profile and flux of large sea-salt particles in a coastal zone. *J. Geophys. Res.*, **106,** 12 039–12 054.

Russell, P. B., P. V. Hobbs, and L. L. Stowe, 1999: Aerosol properties and radiative effects in the U.S. East Coast haze plume: An overview of the Tropospheric Aerosol Radiative Frocing Observational Experiment (TARFOX). *J. Geophys. Res.*, **104,** 2213–2222.

Sakerin, S. M., and D. M. Kabanov, 1997: Some results of shipboard measurements of the aerosol optical thickness at visible and near-IR wavelengths. *J. Aerosol, Sci.*, **28,** S107–S108.

——, D. M. Kabanov, and V. V. Polkin, 1995: Optical investigations of atmosphere during the 35th voyage of the research vessel *Akademik Mstislav Keldysh* (English translation). *Atmos. Oceanic Opt.*, **8,** 1767–1777.

Sakunov, G. G., and Coauthors, 1981: Optical properties of the Arctic atmosphere (in Russian). *Polar Aerosol, Cloudness and Radiation,* Gidrometeoizdat, 73–89.

Sandomirskiy, A. B., M. V. Dyakonova, and G. I. Trifonova, 1971: Radiance functions of the sky and atmospheric transmittance in the 0.28–2.24 mm spectral range (English translation). *Izv. Acad. Sci. USSR Atmos. Oceanic Phys.*, **7,** 261–265.

Satheesh, S. K., K. K. Moorthy, and B. V. Krishna Murthy, 1998: Spatial gradients in aerosol characteristics over the Arabian Sea and Indian Ocean. *J. Geophys. Res.*, **103,** 26 183–26 192.

——, V. Ramanathan, X. Li-Jones, J. M. Lobert, I. A. Podgorny, J. M. Prospero, B. N. Holben, and N. G. Loeb, 1999: A model for the natural and anthropogenic aerosols over the tropical Indian Ocean derived from Indian Ocean Experiment data. *J. Geophys. Res.*, **104,** 27 421–27 440.

Schmid, B., and Coauthors, 1999: Comparison of aerosol optical depth from four solar radiometers during the fall 1997 ARM Intensive Observation Period. *Geophys. Res. Lett.*, **26,** 2725–2728.

——, and Coauthors, 2001: Comparison of columnar water vapor measurements from solar transmittance methods. *Appl. Opt.*, **40,** 1886–1896.

Shaw, G. E., 1980: Transport of Asian desert aerosol to the Hawaiian Islands. *J. Appl. Meteor.*, **19,** 1254–1259.

——, 1983: Sun photometry. *Bull. Amer. Meteor. Soc.*, **64,** 4–10.

Shettle, E. P., and R. W. Fenn, 1979: Models for the aerosols of the lower atmosphere and the effects of humidity variations on their optical properties. *Environ. Res. Pap.*, **676,** 1–100.

Shifrin, K. S., V. A. Gashko, and B. V. Novogrudskiy, 1975: Spectral transmittance of atmosphere over the tropical part of the Indian Ocean (in Russian). *Geophysical Studies in the Indian Ocean,* Nauka, 164–170.

——, O. A. Yershov, E. L. Lysenko, and B. N. Volkov, 1980a: Optical studies of aerosol structure over the island of Kikhnu (in Russian). *Optical Methods of Studying the Oceans and Inland Waters,* K. S. Shifrin, Ed., Tallinn, 244–248.

——, ——, V. M. Volgin, and A. M. Kokorin, 1980b: Maritime aerosol studies based on coastal observation data (English translation). *Izv. Acad. Sci. USSR Atmos. Oceanic Phys.*, **16,** 166–170.

——, V. M. Volgin, B. N. Volkov, O. A. Yershov, and A. V. Smirnov, 1985: Optical depth of atmospheric aerosol over the sea. *Issled. Zemli iz Kosmosa*, **2,** 21–30. (English translation, *Sov. J. Remote Sens.*, **5,** 591–605, 1989.)

Smirnov, A. V., and Y. N. Gulyaev, 1990: The air masses influence on optical characteristics of maritime atmosphere (in Russian). *Tr. Leningr. Gidrometeor. Inst.*, **108,** 110–114.

——, Y. Villevalde, N. T. O'Neill, A. Royer, and A. Tarussov, 1995a: Aerosol optical depth over the oceans: Analysis in terms of synoptic air mass types. *J. Geophys. Res.*, **100,** 16 639–16 650.

——, O. Yershov, and Y. Villevalde, 1995b: Aerosol optical depth in the Atlantic Ocean and Mediterranean Sea. *Proc. SPIE*, **2582,** 203–214.

——, B. N. Holben, I. Slutsker, E. J. Welton, and P. Formenti, 1998: Optical properties of Saharan dust during ACE-2. *J. Geophys. Res.*, **103,** 28 079–28 092.

——, ——, O. Dubovik, N. T. O'Neill, L. A. Remer, T. F. Eck, I. Slutsker, and D. Savoie, 2000a: Measurement of atmospheric optical parameters on U.S. Atlantic coast sites, ships and Bermuda during TARFOX. *J. Geophys. Res.*, **105,** 9887–9901.

——, ——, T. F. Eck, O. Dubovik, and I. Slutsker, 2000b: Cloud screening and quality control algorithms for the AERONET data base. *Remote Sens. Environ.*, **73,** 337–349.

Tanre, D., M. Herman, and Y. J. Kaufman, 1996: Information on the aerosol size distribution contained in the solar reflected spectral radiances. *J. Geophys. Res.*, **101,** 19 043–19 060.

Tavartkiladze, K. A., 1979: Statistical characteristics of spectral optical depth of maritime atmosphere (English translation). *Izv. Acad. Sci. USSR Atmos. Oceanic Phys.*, **15,** 852–855.

Tomasi, C., and F. Prodi, 1982: Measurements of atmospheric tur-

bidity and vertical mass loading of particle matter in marine environments. *J. Geophys. Res.,* **87,** 1279–1286.

Twomey, S. A., M. Piepgrass, and T. L. Wolfe, 1984: An assessment of the impact of pollution on global cloud albedo. *Tellus*, **36,** 356–366.

Villevalde, Y. V., K. S. Lamden, and A. V. Smirnov, 1984: The results of maritime atmospheric spectral transmittance measurements (in Russian). *Abstracts, VIII All-Union Symp. on Laser and Acoustic Soundings of the Atmosphere*, Part 1, Tomsk, Russia, Institute of Atmospheric Optics, 111–113.

——, V. V. Yakovlev, and S. P. Smyshlyaev, 1989: Measurements of atmospheric optical parameters in Baltic Sea and Atlantic Ocean (in Russian). *Studies of the Southern Part of the Norway Sea,* Y. Y. Kluikov et al., Eds., Gidrometeoizdat, 105–110.

——, A. V. Smirnov, N. T. O'Neill, S. P. Smyshlyaev, and V. V. Yakovlev, 1994: Measurement of aerosol optical depth in the Pacific Ocean and the North Atlantic. *J. Geophys. Res.*, **99,** 20 983–20 988.

Viollier, M., D. Tanre, and P. Y. Deschamps, 1980: An algorithm for remote sensing of water colour from space. *Bound.-Layer Meteor.,* **18,** 247–267.

Volgin, V. M., O. A. Yershov, A. V. Smirnov, and K. S. Shifrin, 1988: Optical depth of aerosol in typical sea areas (English translation). *Izv. Acad. Sci. USSR Atmos. Oceanic Phys.,* **24,** 272–277.

Volz, F., 1970: Spectral skylight and solar radiation measurements in the Carribean: Maritime aerosol and Sahara dust. *J. Atmos. Sci.,* **27,** 1041–1046.

von Hoyningen-Huene, W., and A. Raabe, 1987: Maritime and continental air mass differences in optical aerosol extinction. *Beitr. Phys. Atmos.,* **60,** 81–87.

——, and M. Wendisch, 1994: Variability of aerosol optical parameters by advective processes. *Atmos. Environ.* **28,** 923–933.

Voss, K. J., E. J. Welton, P. K. Quinn, R. Frouin, M. Miller, and R. M. Reynolds, 2001: Aerosol optical depth measurements during the AEROSOL99 experiment. *J. Geophys. Res.,* **106,** 20 821–20 832.

Weller, M., and U. Leiterer, 1988: Experimental data on spectral aerosol optical thickness and its global distribution. *Beitr. Phys. Atmos.,* **61,** 1–9.

Whitby, K. T., 1978: The physical characteristics of sulfur aerosols. *Atmos. Environ.,* **12,** 135–159.

Wilson, W. H., 1979: Measurements of atmospheric transmittance in a maritime environment. *Proc. SPIE,* **195,** 153–159.

Wolgin, V. M., V. F. Radionov, and U. Leiterer, 1991: Zur variabilitat der optischen eigenschaften der atmosphare in Nordatlantik. *Z. Meteor.,* **41,** 267–272.

Yershov, O. A., and A. V. Smirnov, 1986: Spectral transmittance of coastal atmosphere, *Issled. Zemli iz Kosmosa*, **3** (5), 3-8. (English translation, *Sov. J. Remote Sens.,* **6,** 687–696 1990.)

——, A. M. Kokorin, and K. S. Shifrin, 1982: Aerosol studies in the tropical zone of the Atlantic ocean (in Russian). *Abstracts, I Congress of Soviet Oceanologists*, Part 1, Sevastopol, Russia, 53–54.

——, A. V. Smirnov, and K. S. Shifrin, 1990: Spectral transparency and solar halo in the atmosphere above the ocean (English translation). *Izv. Acad. Sci. USSR Atmos. Oceanic Phys.,* **26,** 287–292.

Zibordi, G., and G. Maracci, 1988: Determination of atmospheric turbidity from remotely-sensed data: A case study. *Int. J. Remote Sens.,* **9,** 1881–1894.